



UNIVERSITA' DEGLI STUDI DI PISA

*Corso di Dottorato di Ricerca
in
Fisiopatologia e Clinica dell'Apparato Cardiovascolare e Respiratorio*

Tesi

**HYPERTROPHIC CARDIOMYOPATHY:
RELATIONSHIP BETWEEN MYOCARDIAL ISCHEMIA,
FIBROSIS AND CLINICAL STATUS**

Anno Accademico 2012-2013

Candidato

Dott. Giancarlo Todiere

Presidente del Corso

Prof. Alfredo Mussi

Tutors

Prof. Mario Marzilli

Dott. Massimo Lombardi

This manuscript collects some papers (two already published and one other waiting for submission) on hypertrophic cardiomyopathy (HCM) produced during my PhD program, linked together by the same leading thread working to demonstrate the relationship existing between myocardial ischemia and fibrosis, both hallmarks of the disease.

INTRODUCTION

HCM is a genetic disorder that is typically inherited in an autosomal dominant fashion. There are defects in several of the genes encoding for the sarcomeric proteins, such as myosin heavy chain, actin, tropomyosin, and titin. Multiple mutations have been identified, with genotype-specific risks for mortality and degree of hypertrophy . The disorder has a variable clinical presentation and carries a high incidence of sudden death. HCM is the leading cause of sudden cardiac death in young population . However, many patients may remain stable over long periods of time and then suddenly they may present adverse events: unexpected death, embolic stroke, and the consequences of heart failure .

The disease is characterized by an inappropriate myocardial hypertrophy, often asymmetrical, and occurs with no obvious inciting hypertrophy stimulus . Hypertrophy can occur in any region of the left ventricle but frequently involves the interventricular septum, which sometimes results in an obstruction of flow through the left ventricular outflow tract (LVOT) . At histology, myocardial disarray and islands of fibrosis are considered hallmarks of this disease . The systolic function of LV is preserved until the end-stage of the disease, but the thickened myocardium with fibrosis increases the stiffness of LV chamber causing impaired diastolic relaxation which produces atrial enlargement and may promote atrial fibrillation . At the end stage, the loss of myocytes, replaced by gross scar, is sufficient to determine a manifest systolic LV dysfunction . Myocardial scars create a potentially arrhythmogenic substrate and may increase susceptibility to ventricular tachycardias/fibrillation . Indeed, gross macroscopic scarring is frequently present on post-mortem examination in HCM patients who died suddenly, suggesting a possible causal association between fibrosis and malignant arrhythmias .

In most patients with HCM, dense focal myocardial fibrosis can also be visualized noninvasively with the use of gadolinium-enhanced cardiac magnetic resonance imaging (LGE-CMR) . Recently, some studies demonstrated the prognostic role of fibrosis, expressed as late gadolinium enhancement (LGE), as predictor of myocardial death . In addition is also possible to quantify extent of LGE in the myocardium of these patients .

The diagnosis of HCM is usually performed at relatively young age when not significant stenosis are present in the main coronary arteries. Despite this, many studies showed the importance of myocardial ischemia, probably also due to microvascular disease, as cause of myocardial fibrosis and symptoms and as a trigger of ventricular arrhythmias . Infact the assessment of myocardial ischemia in selected patients with HCM (with preserved LV function) may represent a prognostic tool for identifying those patients at risk for profound disease progression.

CMR also allows to evaluate myocardial perfusion and quantify non invasively myocardial blood flow .

It's now clear the importance to study both and individually myocardial fibrosis and ischemia, and to evaluate the relationship between myocardial scar, myocardial blood flow and clinical expression of the disease.

1) Myocardial blood flow and fibrosis in hypertrophic cardiomyopathy

(J Card Fail. 2011 May;17(5):384-91)

In the first study I investigated the relation between myocardial blood flow (MBF), fibrosis, risk factors for sudden death and clinical manifestations in HCM. To strengthen the relationship between microvascular abnormalities and myocardial fibrosis I performed the analysis on two different models of hypertrophy: HCM and cardiac acromegalic population study, as a model of organized myocardial hypertrophy, without disarray and, as we previously demonstrated, with the absence of detectable LGE. Therefore the purposes of the study were: a) to evaluate the association between MBF and the extent of fibrosis in patients with HCM by cardiac magnetic resonance (CMR); b) to assess the relation between MBF and fibrosis with "clinically established" risk factors for sudden death; c) to demonstrate the role of a reduced MBF and the presence of LGE in HCM for the occurrence of symptoms. CMR with velocity-encoded phase contrast technique (PC-CMR) is a validated method to quantify blood flow. Coronary sinus blood flow constitutes 96% of the total venous drainage of coronary blood flow. Thus, quantification of coronary sinus flow by PC-CMR is an alternative way to assess myocardial blood flow (MBF) without exposing patients to ionizing radiation. Previous studies demonstrated excellent agreement between myocardial PET and PC-CMR for the quantification of MBF.

METHODS

Patient Population

A total of 64 consecutive patients with HCM (45 males, mean age of 47 ± 16 years) were enrolled in the study from January 2007 to June 2009. The diagnosis of HCM was based on previously-reported criteria.

As a model of left ventricular hypertrophy non-HCM, we included patients with cardiac acromegaly: from an initial population of 35 consecutive patients with untreated active acromegaly who underwent CMR, we selected 15 patients (9 male, 47 ± 12 years old) having left ventricular mass index higher than the referral range. Twenty healthy, normal subjects (14 males, mean age of 48 ± 10 years) were enrolled as a control group.

To exclude the presence of coronary artery disease, we included in HCM and in acromegalic population patients with a negative coronary angiography, or a negative exercise test or a low (<10%) 10-year risk for coronary events. The study was approved by the internal ethical committee of our institute.

The following markers of increased risk of sudden death in patients with HCM were evaluated: family history of sudden death, extreme left ventricular (LV) wall thickness (≥ 30 mm), unexplained (non vasovagal) syncope, and non-sustained ventricular tachycardia (VT) on ambulatory ECG Holter recordings (> 4 ventricular beats). By clinical interrogation, each patient was classified in a NYHA class, assessed by a physician blinded to CMR data, on the basis of the presence and the severity of dyspnea before the CMR examination. The history of other symptoms (chest pain, palpitation) was also recorded. A 12-lead resting electrocardiogram was recorded on the day of the CMR examination. The presence of LV outflow tract obstruction was evaluated by echocardiography and defined as an LV outflow gradient ≥ 30 mmHg.

Magnetic Resonance acquisition protocol

CMR study was performed with a dedicated 1.5 Tesla (Signa Hdx, General Electric Healthcare, Milwaukee, Wisconsin) with a 8 channel cardiac phased array coil.

Short axis cine images from the mitral plane valve to the left ventricular apex were acquired using a steady-state free precessing (FIESTA) pulse sequence with the following parameters: 30 phases, slice thickness 8 mm, no gap, views per segment 8, NEX 1, FOV 40 cm, phase FOV 1, matrix 224x224, reconstruction matrix 256 x 256, a 45° flip angle, TR/TE equal to 3.5/1.5, and a bandwidth of 125 KHz.

Coronary sinus flow was obtained acquiring images orthogonal to the coronary sinus, using imaging planes as close as possible to the right atrium, to include as many posterior cardiac veins as possible. A free breathing velocity-encoded phase contrast gradient-echo cine sequence with cardiac and respiratory gating was used. The following parameters were applied: TR/TE 12/5 msec, flip angle 20°, field of view 30, phase field of view 1, matrix 192x160, reconstruction matrix 256x256, slice thickness 5 mm, number of excitation 5. Flow sensitivity was set to 50 cm/sec of encoded velocity and raised if aliasing artifact occurred. By the respiratory gating the image data were phase reordered to minimize respiratory artifact. The use of free breathing velocity-encoded phase contrast technique was previously validated by the comparison with flow probe measurement in coronary sinus and in coronary artery .

LGE technique was used to evaluate the extent of myocardial necrosis. LGE images were acquired in short axis views from mitral plane valve to the left ventricular apex by a 2D segmented inversion-recovery-prepared gradient echo pulse sequence.

Images were acquired 10 minutes after administration of Gd-DTPA (Magnevist, Schering-AG) with a dosage of 0.2 mmol/kg in short axis views. The following parameters were used: field of view 40

mm, slice thickness 8 mm, no gap between each slice, repetition time 4.6 msec, echo time 1.3, flip angle 20°, matrix 224 x 192, reconstruction matrix 256 x 256, number of excitation 1, R-R interval 2. The appropriate inversion time was set to null normal myocardium (range 250-350 milliseconds).

At the end of the examination, a phantom was placed in the CMR scanner and a velocity-encoded fast contrast gradient-echo cine sequence was acquired with the same acquisition plane and parameters used for the patient .

Image post-processing

Analysis of MRI images was performed using a commercially available research software package (Mass Analysis, Leyden, The Netherlands). Left ventricular (LV) mass was measured by the analysis of the cine short axis images. The endocardial and epicardial contours of LV myocardium were traced in the end-diastolic and the end-systolic phase. End-diastolic volume index (EDVi), end-systolic volume index (ESVi) and mass index were measured as previously described .

The volumetric data of LV and right ventricle (RV) were plotted against the time (in msec) in a volumetric filling time curve. LV diastolic parameters were calculated from the volumes/time curve as previously described . Briefly, a dV/dT curve was generated as the first derivative transformation of the volumetric filling time curve. The early (E) and late (A) peak filling rate (PFR) were measured in dV/dT curve as, respectively, the early and the late diastolic peak of dV/dT curve. The PFR E/ PFR A ratio was defined as the ratio between the early and the late peak filling rate.

Mitral regurgitant volume was measured as the difference between LV and RV stroke volumes.

Coronary sinus flow was measured as previously described . Briefly, the coronary sinus contour was traced first on the magnitude images at each cine frame. Then the traced region of interest was applied on the corresponding phase image (figure 1). The effect of through-plane motion caused by cardiac contraction in the oblique coronary plane was relatively small. However, phase-offset errors were minimized, for each cardiac phase, by subtracting the signal from the phase images acquired in the phantom at the end of the CMR examination. Cross-sectional area of the coronary sinus was measured in the magnitude images throughout the cardiac cycle. Mean flow velocity of coronary sinus was obtained in the respective phase image. Blood flow was calculated as the product of area and mean flow velocity in each cardiac phase. Coronary sinus was multiplied for the heart rate, obtaining the coronary sinus flow/minutes. The MBF was calculated as coronary sinus flow/minutes divided by LV mass and expressed as ml/min/g.

The extent of LGE was measured as previously described . A region of interest (ROI) was selected in the background of the image. Mean signal intensity and standard deviation (SD) of this ROI were measured. The LV myocardium was delimited by endocardial and epicardial contours traced manually. Enhanced myocardium was defined as myocardium with a signal intensity of ≥ 6 SDs above the mean of the ROI. The extent of LGE was expressed as percentage of the LV mass. LGE was defined undetected when the measured extent was $<0.1\%$ of LV mass.

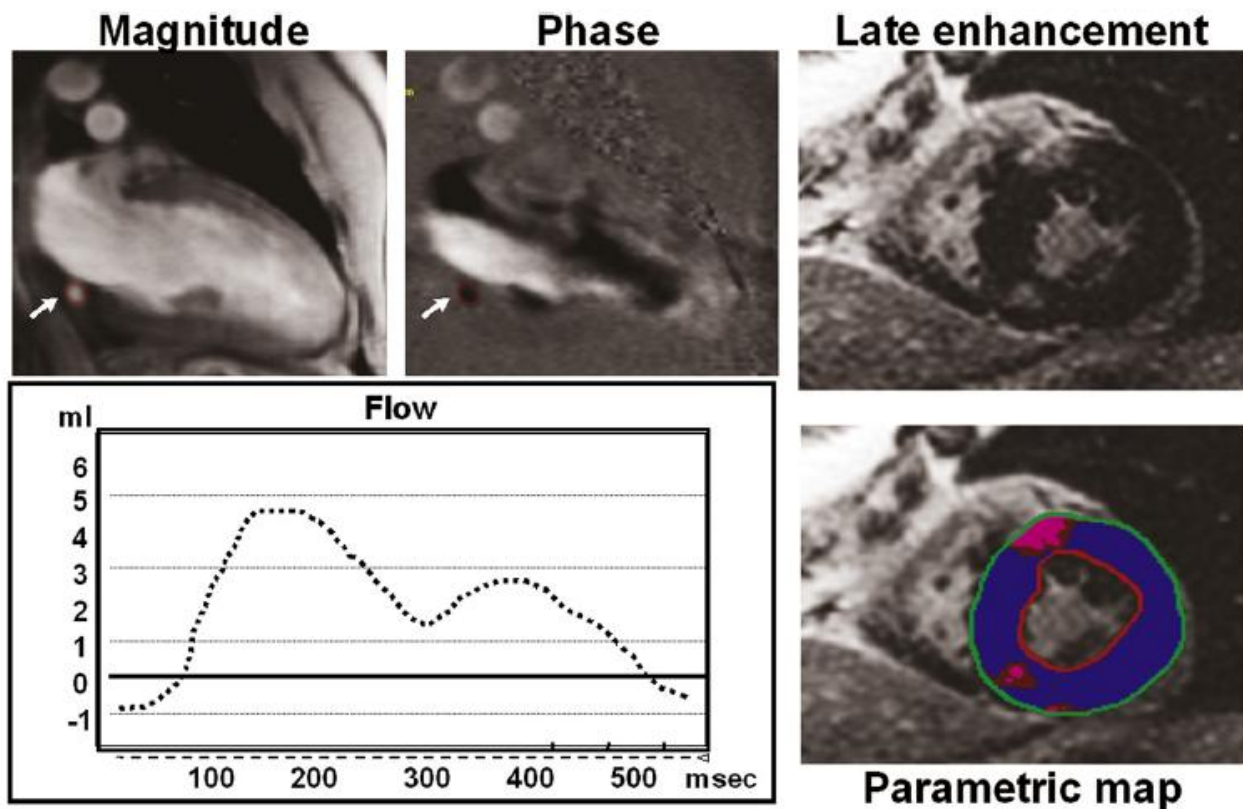


Figure 1. Coronary sinus flow measurement. Cross-sectional coronary sinus area was traced in all of the magnitude images (top left), and identical area is automatically traced in phase images (top middle). Blood flow was calculated as the product of cross-sectional area and mean flow velocity in each cardiac phase (bottom left). In the same patient, areas of late gadolinium enhancement were detected, as evidenced in a short-axis image (top right) and in its parametric map (bottom right).

Statistical analysis

All data were analysed using JMP® software (version 4.0). Data are presented as continuous variables and proportions (percentages). Continuous variables are expressed as means \pm 1 SD. Categorical variables were compared by Pearson chi-square test or Fisher's exact test when appropriate. One-way analysis of variance or Bonferroni post-hoc test, when appropriate, were used to compare quantitative variables across groups. A p value <0.05 was considered statistically significant. A multiple regression analysis, including MBF as dependent and the presence of LGE, the extent of LGE, the maximal end-diastolic wall thickness, history of atrial fibrillation and the age as independent variables, was performed with a stepwise selection procedure to assess the predictors of MBF in HCM population. Logistic regression analysis with a stepwise selection procedure ($p < 0.05$ for entry; $p > 0.10$ for removal) was used to evaluate the influence of covariates on NYHA class $>I$. A Bland-Altman plot was used to evaluate the inter-observer reproducibility of the MBF measurement (figure 2) performed by two blinded observers.

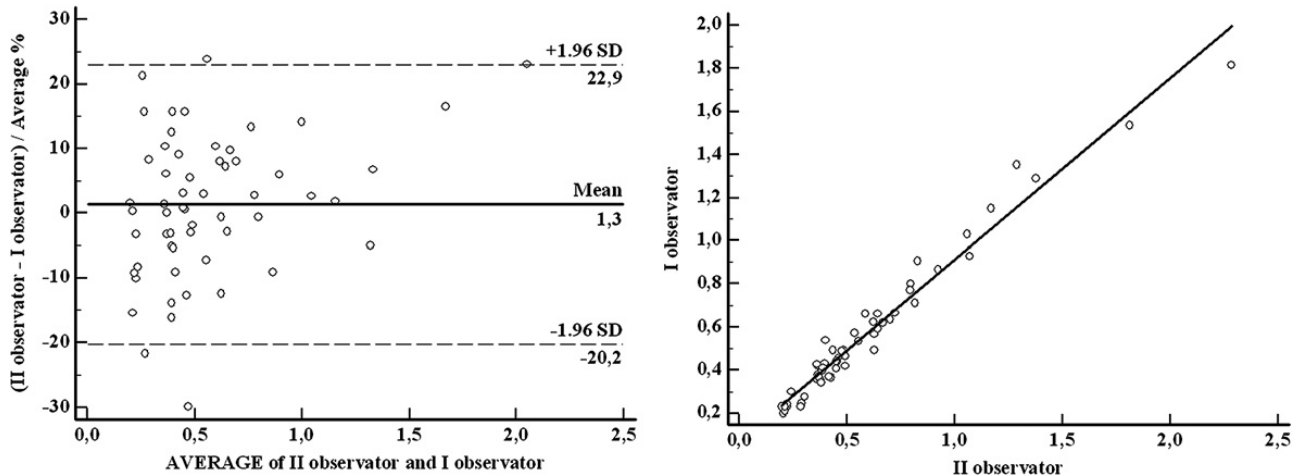


Figure 2. Bland-Altman plot for the interobserver reproducibility of the measurement of myocardial blood flow (left) and the scatter diagram (right panel) showed good agreement between the observers.

RESULTS

The clinical characteristics of the HCM patients are summarized in Table 1. Coronary angiography was performed in 35 patients. Ischemic provocative test was performed in 12 patients. In 17 patients, aged <30 years, with an estimated risk of coronary artery disease lower than 10%, no ischemic provocative test were performed. Two patients were excluded because of the presence of coronary artery disease, found by angiography. The final population included 62 patients with HCM. In the acromegalic patients mean serum GH and IGF-1 concentrations were 7.1 ± 9.9 $\mu\text{g/l}$ and 736 ± 222 $\mu\text{g/l}$, respectively. As evidenced in table 1, LV mass index was significantly higher in HCM than in controls but not significant different between HCM and acromegaly patients.

Acromegaly patients had higher LV mass index than controls (92 ± 30 vs 74 ± 25 g/m^2 , $p<0.05$).

Resting MBF was significantly lower in patients with HCM than in controls (0.56 ± 0.28 vs 0.92 ± 0.5 ml/g/min , $p<0.04$, figure 3). MBF was also significantly lower in patients with HCM than in acromegaly patient.

LGE was detected in 39(63%) patients with HCM and in none of the acromegalic patients and controls. HCM patients with and without detectable LGE were similar for age (respectively 45 ± 14 vs 48 ± 18 years, $p 0.45$) and gender (male 71% vs 73 % respectively). MBF was lower in HCM patients with positive LGE than in those with negative LGE (0.46 ± 0.2 vs 0.66 ± 0.29 ml/g/min $p0.005$) (fig. 3B). Patients in HCM group without LGE had lower MBF than controls ($p 0.04$). For multiple regression analysis the independent predictors of MBF were the presence of LGE ($p 0.03$, coefficient $-0,025$) and the LV mass index ($p 0.012$, coefficient $-0,004$).

Table 1: Clinical variables of the HCM population

Variables	Controls	p value*	HCM	p value**	Acromegaly
number	20		62		15
Age (years)	48±10	0.79	47±16	0.99	47±12
Male (n)	14(70%)	0.94	45(72%)	0.52	9(60%)
Familiar history of HCM n(%)	-		6(10%)		-
Risk factors for SCD n(%):					
Familiar history of SD	-		3(5%)		-
Maximal wall thickness ≥30mm	-		1 (2%)		-
Outflow pulse gradient >30 mmHg	-		15 (24%)		-
Unexplained syncope	-		4(6%)		-
VT at 24-Holter monitoring	-		10(16%)		-
Clinical manifestation n(%):					
Angina	-		15(24%)		-
Palpitation	-		15(24%)		-
Dyspnea NYHA class ≥II	-		41 (66%)		-
NYHAclass II			38(61%)		
NYHA class III			3(5%)		
History of atrial fibrillation	-		9(44%)		-
CMR findings:					
Maximal end-diastolic thickness (mm)	8±3	<0.0001	20±5	<0.0001	13±8
LV mass (g)	129±30	<0.0001	197±54	0.06	167±60
LV mass index (g/m ²)	74±25	0.01	104±28	0.18	93±30
LV end-diastolic volume index (ml/m ²)	86± 11	0.5	80± 16	0.24	85±9
LV ejection Fraction (%)	64±5	0.06	69±8	0.18	66±7
LV ejection Fraction <50% n(%)	0		4(6%)		0
Extent of LGE (% of LV mass)	0		9.4±13.5		0
MBF (ml/min/g)	0.92±0.5	0.04	0.56±0.28	<0.0001	1.36±0.5
Therapy n(%):					
			26 (42%)		
Beta blockers	-		21(34%)		-
Calcium-antagonist	-		4(6%)		-
ACE-inhibitors	-		7(11%)		-
Diuretic	-		5(8%)		-
Anti-arrhythmic	-		1(1.6%)		-

HCM, hypertrophic Cardiomyopathy; SCD, sudden cardiac death; VT, ventricular tachycardia; ACE, angiotensin converting enzyme; LGE, late gadolinium enhancement; MBF, myocardial blood flow; * p value controls vs HCM; ** p value of HCM vs acromegalic patients.

Risk factors and MBF

MBF was not significantly different in patients with than in those without family history of sudden cardiac death (0.41 ± 0.07 vs 0.57 ± 0.3 ml/g/min, p 0.31). Patients with unexplained syncope had significantly higher MBF (0.91 ± 0.1 vs 0.55 ± 0.3 ml/g/min, $p < 0.02$). MBF was lower in patients with at least one risk factor than in patients without any risk factors (0.48 ± 0.27 vs 0.63 ± 0.27 ml/g/min, $p < 0.05$).

At 24 hours ECG Holter monitoring VT was recorded in 10 (16%) patients. As showed in table 2 patients with VT had significantly lower MBF than patients without. Yet, patients with non-sustained VT had significantly higher extent of LGE, higher maximal end-diastolic thickness and total risk score.

Table 2: Occurrence of VT in population with HCM

Variables	Non-sustained VT	Absence of non-sustained VT	p-value
Patients	10	52	
Male	7 (70%)	37(74%)	
Age (year)	53 ± 12	46 ± 16	0.09
Risk factors for SCD:			
Familiar history of SCD	0	3 (5%)	
Unexplained syncope	3 (5%)	0	0.5
Maximal end-diastolic wall thickness (mm)	23 ± 3	19 ± 5	0.05
Outflow pulse gradient (mmHg)	16 ± 25	15 ± 26	0.9
Total risk score(n. of risk factor per SCD)	1.6 ± 0.9	0.4 ± 0.6	<0.01
CMR:			
Extent of LGE (% of LV mass)	29.3 ± 4.5	7.3 ± 1.9	<0.0001
MBF (ml/g/min)	0.4 ± 0.14	0.6 ± 0.29	<0.04
LV mass index (g/m ²)	109 ± 24	104 ± 29	0.9
LV ejection fraction (%)	66 ± 11	70 ± 8	0.34
PFR E (ml/sec)	319 ± 169	398 ± 280	0.5
PFR A (ml/sec)	211 ± 101	229 ± 95	0.7
PFR E/PFR A	3.4 ± 4.1	1.9 ± 1.2	0.2

VT, patients with episode of ventricular tachycardia at 24-hours Holter monitoring; no-VT, patients without episode of ventricular tachycardia; SCD, sudden cardiac death; LGE, late gadolinium enhancement; MBF, myocardial blood flow; LV, left ventricle; PFR E, peak of filling rate E; PFR A peak of filling rate A.

Clinical Manifestations and MBF

The incidence of symptoms in the total population of HCM is showed in table 1. Of the HCM population 38 patients were in NYHA class II, 3 in class III e none in class IV. However, average MBF was 0.44 ± 0.22 ml/g/min for patients in NYHA class II and 0.43 ± 0.2 ml/g/min in class III.

Compared with asymptomatic patients, MBF was not different in patients with angina (0.61 ± 0.32 vs 0.57 ± 0.26 ml/g/min, p 0.8), palpitations (0.61 ± 0.32 vs 0.61 ± 0.3 ml/g/min, p 0.99) and history of atrial fibrillation (0.61 ± 0.32 vs 0.57 ± 0.2 ml/g/min, p 0.7). In table 3 the clinical and CMR parameters of HCM patients with preserved LV function (ejection fraction $\geq 50\%$) are reported. This selection of patients have been done to assess the role of reduced MBF and the presence of fibrosis in absence of LV dysfunction, as potential cause of dyspnea. In this selected group of HCM patients, those in NYHA functional class \geq II had lower MBF than patients in NYHA class I.

Moreover, the patients in NYHA class \geq II showed a larger extent of LGE, higher maximal end-diastolic wall thickness, greater left atrium and higher mitral regurgitant volume than the patients in NYHA class I. Furthermore, the patients in NYHA functional class \geq II had significantly lower PFR A. In the logistic regression model, including MBF, extent of LGE, age, maximal LV wall thickness and left atrial diameter, MBF was the only independent predictor of NYHA $>$ I (coefficient 5.8, standard error 2.37, p 0.01).

DISCUSSION

The main results of this study could be synthesized as follows: 1) resting MBF was significantly lower in HCM than in controls and in patients with acromegalic LV hypertrophy; 2) patients with HCM presenting fibrosis as detected by LGE showed lower MBF than those without; 3) an association between non-sustained VT and MBF was found in this population 4) MBF was the only independent predictor of worse functional class (NYHA class \geq II).

Resting MBF in HCM

Kawada et al. evaluated MBF by PC-CMR in 29 patients with HCM in resting condition and during hyperemia induced by dipyridamole. They demonstrated a reduced hyperemic response to vasodilator in HCM patients than in controls, with a non significant difference in resting MBF. The results of the current study showed that basal MBF was significantly lower in HCM than in healthy controls. This could be explained because of the larger size of population in our study than in the previous one. Moreover, the selection of patients was different: we enrolled also patients with previous history of atrial fibrillation and/or impaired ejection fraction which were excluded in the previous study. Patients with HCM complicated by episode of paroxysmal atrial fibrillation or by

decreased EF could be in advanced stage of disease and have lower MBF than those without. The finding of a decreased MBF is concordant with the physiopathologic mechanism of ischemia in HCM. In fact, a mismatch between disproportionate LV hypertrophy, lack of capillary growth, and abnormally narrowed intramural coronary arteries, were previously demonstrated in HCM and could be used to partially justify the reduced supply of blood flow at rest . Myocardial fibrosis could participate to the decruitment of capillary vessels, and be involved in decreasing resting MBF. Alternatively, replacement fibrosis could be secondary to brief episodes of repeated ischemia.

In this study the presence of detectable LGE and the LV mass index were independent predictors of MBF in HCM. The mismatch between the coronary flow supply and the increased LV mass may result in a reduction of global MBF. The disproportion between increased mass and flow was an intrinsic feature of HCM as demonstrated by the comparison with acromegalic LV hypertrophy . We chose LV hypertrophy in acromegaly because it is a model of organized myocardial hypertrophy, without disarray and, as we previously demonstrated, with the absence of detectable LGE .

In age- and sex-matched patients with acromegaly and LV hypertrophy a significant lower maximal wall thickness than in HCM was found although the LV mass index was not different. Despite similar LV mass index, significant higher MBF than HCM was measured. Then, in acromegaly the increased LV mass index was balanced by a proportionate increase in coronary flow resulting in a preserved MBF.

In this study we found an association between myocardial fibrosis detected by LGE technique and MBF: patients with HCM and a positive LGE had significantly lower MBF than those with negative LGE. These results suggest a link between fibrosis and MBF, even if it remains unclear whether fibrosis is a consequence of myocardial ischemia or it is a direct cause of reduced MBF at rest.

Resting MBF and ventricular arrhythmias

Both myocardial fibrosis and transitory ischemia were considered as potential substrate in triggering malignant ventricular arrhythmias . In agreement with previous reports, results of the current study confirmed the relation between total risk score, the maximal end diastolic wall thickness, and the extent of LGE with ventricular tachyarrhythmias on 24 hours ECG monitoring . Moreover, we found that patients with episode of non-sustained VT had significantly lower MBF at rest and higher extent of LGE. The occurrence of episodes of non sustained VT at 24 Holter ECG monitoring is generally regarded to be an independent determinant of increased risk of sudden

death in this disease . Thus, these results highlight the value of LGE as an emerging feature to be evaluated in patients with HCM. LGE could be particularly useful to stratify the risk in subjects with only one “accepted” risk factor of sudden death .

Recently, two large studies evaluated the prognostic role of LGE in HCM demonstrating that patients with a positive LGE had worse prognosis than those without a detectable LGE . However, LGE was described in most of HCM patients (60-80% of them) and it may be considered a sensitive predictor of worse outcome also taking into account other parameters such as LGE extent, the pattern of distribution of LGE, and also the MB to stratify more accurately patients with HCM. Thus, the impact on the clinical management and the prognostic role of resting MBF in HCM should be evaluated by further long-term follow-up studies.

Resting MBF and NYHA class

A significant correlation between LGE and impaired functional class (NYHA class \geq II) has been already demonstrated . In this study we also found a reduced MBF in patients with impaired NYHA class. The presence of atrial dilatation, the maximal wall thickness and a reduced PFR E were also associated to worse NYHA class. Noteworthy, only MBF was an independent predictor of worse functional class. Therefore, it is hypothesizable that effort dyspnea could be secondary to brief episodes of ischemia, already documented in HCM patients, and that ischemia could more likely occur in patients with a low resting MBF.

Moreover, previous study showed that subject with impaired MBF were more likely to experience LV remodeling with dilatation, wall thinning and systolic dysfunction .

Study limitations

The main limitation to the current study was the absence of evaluation of MBF during hyperemia. However, our results suggest that the evaluation of resting MBF could be useful for the clinical stratification in patients with HCM. The prognostic role of impaired resting MBF and coronary reserve must be evaluated by further long-term follow-up studies.

Flow measurement in this study was performed using a free breathing velocity-encoded phase contrast pulse, which has been previously validated invasively by the comparison with the flow probe measurements of coronary sinus and coronary arteries . Although vessel contours may be blurred with this approach owing to motion artifacts, in same time, the potential of using multiple averages (NEX = 5) increases signal-to-noise ratio thus improving image quality. Yet, flow evaluation during free breathing acquisition may be considered more physiological than the acquisition during long breath-holding. Moreover, as showed in table 1, most of the HCM patients

assumed beta-blockers or calcium antagonist therapy and the heart rate was usually around 50-60 bpm. In these patients the acquisition time of the phase-contrast images was longer, lasting usually >25 seconds and some patients may not be able to keep a complete breath-holding. Regarding the ability of velocity-encoded phase contrast imaging CMR to measure flow specifically in small structures. Hofman et al demonstrated that accurate blood volume flow rates may be determined through small vessel for a number of voxels per vessel diameter value of about ≥ 3 . In the present study, we found an average coronary end-systolic diameter of 9 ± 2 mm and end-diastolic diameter of 6 ± 1 mm. Coronary sinus cross section is usually ovoid and the minor diameter is usually oriented in superior-inferior direction and the maximal diameter is anterior-posterior. In our protocol of acquisition of coronary sinus images, the frequency direction is usually in the superior-inferior direction and the phase in anterior-posterior in order to avoid the wrap-around artifact. Thus, despite a voxel dimension of 1.6 mm x 1.9 mm, the number of voxels in each direction is usually >3 . Moreover, the net flow in coronary sinus is mostly evidenced during the cardiac phase when the coronary sinus has a larger diameter. Then, the resulting effect of low spatial resolution may be minimal. The coronary sinus diameters in this study was slightly higher than those found by van Rossum et al. but this may be secondary to the difference in age of population, older in our study, or to the improved quality of cine images with 1.5T scanner.

CONCLUSIONS

CMR may be considered a valuable imaging tool in HCM allowing accurate evaluation of cardiac morphology, quantitative measurement of LV mass, wall thickness, detection and quantification of fibrosis and the quantification of MBF in resting and hyperemic condition. Moreover, CMR is a non invasive, virtually safe technique, without administration of ionizing radiation. Thus, CMR may be particularly important for an initial evaluation of patients with a new diagnosis of HCM, and for serial evaluation of the progression of this disease.

2) Progression of myocardial fibrosis assessed with cardiac magnetic resonance in hypertrophic cardiomyopathy.

(J Am Coll Cardiol. 2012 Sep 4;60(10):922-9)

After the demonstration that during resting conditions patients with myocardial fibrosis had more reduced coronary blood flow than those without, I hypothesized that abnormal MBF, caused by microvascular dysfunction, was responsible for myocardial ischemia-mediated myocyte death, and ultimately for repair in the form of replacement fibrosis. Therefore, I have speculated that myocardial fibrosis is a progressive, and not static phenomenon. In addition, considering the prognostic role of fibrosis in HCM, it is fundamental to understand this pathological process.

Objectives of this second study were: a) to assess the amount and rate of progression of LGE by two consecutive CMR examination ; b) to evaluate the relationship between the rate of progression of LGE and clinical variables.

METHODS

Population

We enrolled a total of 70 consecutive patients with a diagnosis of HCM, in sinus rhythm without contraindications for CMR. All these patients underwent to a first CMR examination (CMR-1). After CMR-1, 15 patients were excluded: 2 patients for known significant coronary artery disease, 8 patients for ICD implantation, 2 patients for permanent atrial fibrillation (occurred after CMR-1), 1 patient for septal myectomy, and finally 2 patients for non-sufficient quality of images. The final population who completed the serial CMR examinations were 55 patients . The study was approved by the internal ethical committee of our institute and all subjects gave their written informed consent. The authors of this manuscript have certified that they comply with the Principles of Ethical Publishing in the International .

All the patients enrolled underwent clinical, electrocardiographic, and echocardiographic evaluation at the time of the CMR-1 and CMR-2. The diagnosis of HCM and assessment of the LV outflow gradient were based on previously reported echocardiographic criteria . The conventional primary prevention risk markers for sudden death in HCM were evaluated: family history of sudden death, extreme left ventricular (LV) wall thickness (> 30 mm), unexplained (non vasovagal) syncope, and non-sustained ventricular tachycardia on ambulatory ECG Holter recordings (> 4 ventricular beats at a heart rate > 120 beats per minute), abnormal "flat" systolic arterial pressure during exercise stress test . A complete clinical evaluation was performed at the enrolment and

repeated at CMR-2. By clinical interrogation, each patient was classified in a NYHA class on the basis of the presence and the severity of dyspnoea. The history of other symptoms (syncope, chest pain, palpitation) was also recorded. A 12-lead resting electrocardiogram was recorded on the day of the CMR examination. An imaging stress test was performed in all the patients. When the stress test was positive, evaluation of coronary anatomy was performed by angiography or coronary computed tomography angiography. Patients with significant coronary artery disease were excluded from the study.

CMR protocol

CMR was performed with a dedicated 1.5 Tesla (Signa Hdx, General Electrics Healthcare, Milwaukee, Wisconsin) with an 8 channel cardiac phased array coil. Short axis cine images from the mitral plane valve to the LV apex were acquired using a steady state free precessing (FIESTA) pulse sequence with the following parameters: 30 phases, slice thickness 8 mm, no gap, views per segment 8, NEX 1, FOV 40 cm, phase FOV 1, matrix 224x224, voxel dimensions 1.78x1.78x8 mm, reconstruction matrix 256 x 256, a 45° flip angle, TR/TE equal to 3.5/1.5, and a bandwidth of 125 KHz. In both the first and second examinations, LGE images were acquired 10 minutes after the administration of Gd-DTPA (Magnevist, Schering-AG) with a dosage of 0.2 mmol/kg in short axis views. An inversion recovery T1-weighted GRE was used with the following parameters: field of view 40 mm, slice thickness 8 mm, no gap between each slice, repetition time 4.6 msec, echo time 1.3, flip angle 20°, matrix 224 x 224, reconstruction matrix 256 x 256, number of excitation 1. The appropriate inversion time was set to null normal myocardium (range 250-300 milliseconds) and it was the same for both CMR examination.

Image analysis

Analysis of CMR images was performed, using a commercially available research software package (Mass 6.1, Leiden, The Netherlands). Left ventricular (LV) mass was measured by the analysis of the cine short axis images. The endocardial and epicardial contours of LV myocardium were manually traced in the end-diastolic and the end-systolic phase. End-diastolic volume index (EDVi), end-systolic volume index (ESVi), mass and mass index were measured as previously described . Maximal LV end diastolic wall thickness was measured as previously described . Comparing the two CMR examination, a significant change in LV mass was defined for a measured difference ≥ 5 grams. The extent of LGE was measured using a previously validated method . Briefly, endocardial and epicardial contours in each image were manually traced to identify LV myocardium in each image. To obtain the standard deviation of the signal noise of the images a region of interest was

placed in the background of the image, near the patient's thoracic wall. The mean signal intensity and standard deviation were measured in this region of interest.

Myocardial voxels with signal intensity higher than the average signal intensity of the region of interest plus 6 standard deviations were considered enhanced. The percentage of enhanced voxels in the entire LV myocardium was measured. Extent of LGE was expressed in gram and percentage of LV mass. A significant increase of LGE was defined when the extent of LGE increased of ≥ 1 gram at CMR-2. This threshold was chosen because in considering the dimensions of the voxel, 1 gram of LGE was equivalent to >50 voxels. The rate of progression of LGE (LGE-rate) was defined as the ratio between the increment of LGE extent in grams and the time (months) between the two examinations. Quantification of LGE was performed in a random fashion by 2 investigators who were blinded to: 1) the clinical information of the patients; 2) the value of LGE extent measured at CMR-1.

Statistical Analysis

Categorical variables were compared by Pearson's chi-squared test or Fisher's exact test as appropriate; the McNemar and the Cochran's tests were employed for analyzing changes in patients' proportions among classes (e.g. NYHA classes) between CMR-1 and CMR-2. Statistical tests used to compare groups included paired/unpaired Student's t test for difference in mean values and Mann-Whitney U test or Wilcoxon's test for skewed variables.

The Pearson's correlation coefficient was employed for quantifying the relationship between Gaussian distributed variables; for skewed variables, the logarithmic transformation was applied (e.g. LGE values). Simple and multiple linear regression analyses were then conducted for quantifying the effect of parameters at CMR-1 in relation to LGE changes at CMR-2. The Kolmogorov-Smirnov test was employed to assess normality of data distribution and for the residuals of regression models. A p-value <0.05 was considered statistically significant.

Data are presented as mean \pm standard deviation (SD), median and interquartile range (IQR) and as proportions with percentage, as indicated. Statistical analyses were performed using Matlab (MathWorks, Natick, MA, USA).

RESULTS

Population

The final population of patients with HCM who completed the serial CMR examinations included 55 patients. The average interval between CMR-1 and CMR-2 was 719 ± 410 days.

Clinical characteristics of the study population are summarized in Table 1.

Thirty-seven patients were males. Age ranged from 14 to 83 years, mean 42.4 ± 17.7 years.

Of the 55 patients, thirty-five (63.6%) were in NYHA functional class I, 19 (34.5%) in class II and 1 (1.8%) in class III at the time of the first CMR evaluation. HCM was obstructive in 5 patients (9%). Ten patients had ≥ 2 arrhythmic risk factors. Three patients had a stress imaging test positive for inducible ischemia despite a coronary artery angiography without significant stenosis in the epicardial coronary arteries.

Table 1: clinical variable of the population in CMR-1 and CMR-2

Clinical variables		CMR-1	CMR-2	p value
Patients	N	55	55	-
Symptoms	N(%)			
Syncope		3(5)	3(5)	-
Angina		12(22)	12(22)	-
Effort dyspnea (NYHA ≥II)		12(22)	20(36)	0.11
Palpitation		12(22)	16(29)	0.5
Arrhythmic risk factors	N(%)			
Patients with 0 risk factor		28(51)	27(50)	-
Patients with 1 risk factor		7(13)	6(12.5)	0.99
Patients with ≥2 risk factors		10(18)	11(20)	0.99
Maximal end-diastolic wall thickness ≥30		3(5)	4(7)	0.99
Unexplained Syncope		3(5)	3(5)	-
VT at 24 hours Holter monitoring		7(13)	9(16)	0.8
Family History of sudden death		4(7)	4(7)	-
Outflow pulse gradient >30 mmHg		5(9)	6(12.5)	0.99
Abnormal Pressure Response during effort		1	1	-
Morphofunctional abnormalities:				
History of paroxysmal atrial fibrillation		5(9)	7(13)	0.99
Atrial dilatation		17(31)	17(31)	0.99
Reduced ejection fraction (<50%)		1	1	-
Mitral regurgitation (>mild)		3(5)	3(5)	-
CMR findings:				
LV mass index (g/m ²)	mean±SD	109.0 ± 23.1	113.1 ± 26.8	0.036
Maximal end-diastolic thickness (mm)	mean±SD	20.8 ± 5.4	21.7 ± 6.1	0.506
Ejection fraction (%)	mean±SD	68.9 ± 9.6	68.5 ± 9.4	0.923
End Diastolic Volume index (ml/m ²)	mean±SD	75.5 ± 17.5	74.5 ± 16.5	0.075
LGE detectable	N(%)	45 (81.8%)	53 (96.4%)	0.031
LGE extent (in grams)	mean±SD	13.3 ± 15.2	24.6 ± 27.5	<0.001
	median (IQR)	8 (15)	17 (30)	<0.001
LGE extent (% of LV mass)	mean±SD	6.2 ± 6.6	10.5 ± 10.0	<0.001
	median (IQR)	4 (7)	8 (12)	<0.001
Therapy:	N(%)			
Beta-blockers		27 (50%)	32(58)	0.8
Calcium antagonist		5 (9.1%)	2(5)	0.99
ACE inhibitors		3 (5.5)	4(10)	0.99
Diuretic		1 (1.8)	1(1.8)	-

VT, ventricular tachycardia; LV, left ventricular, LGE, late gadolinium enhancement; ACE, angiotensin converting enzyme.

CMR-1

Measurements obtained at the initial CMR are summarized in Table 1. At CMR-1, LV mass index was upper the range of normality in 43 (78.2%) of the study patients. The mean maximal end-diastolic wall thickness was 20.8 ± 5.4 mm (range 15-38 mm) and was ≥ 30 mm in 3 patients (5.5%). Myocardial hypertrophy mainly involved the interventricular septum and/or the anterior free wall in 32 (58.2%) patients of the study population. Hypertrophy was confined in the ventricular apex in 10 patients (18.2%) and to the inferior and/or inferolateral wall in 3 patients (5.5%). Finally, hypertrophy was diffuse in 10 patients (18.2%). Mean LV end diastolic volume index was 75.5 ± 17.5 ml/m². Mean LV ejection fraction was $68.9 \pm 9.6\%$, and was $\leq 50\%$ in only one patient (ejection fraction = 37%).

LGE was detected in 45 (81.8%) of the study patients. The mean extent of LGE was 13.3 ± 15.2 grams (median and IQR: 8 and 15 grams, range: 1.2 – 84 grams) with a non-Gaussian distribution ($p < 0.001$). On average, LGE was identified in 2.3 ± 1.9 (range 0-6 segments) of the 16 conventional myocardial segments into which the myocardium was subdivided.

CMR-2

Measurements obtained at the CMR-2 are summarized in Table 1. LV mass augmented in 30 patients (54.5%), remained substantially unchanged in 21 (38.2) and decreased in 4 patients (7.3%) (Figure 1). The mean extent of LGE increased from 13.3 ± 15.2 grams at CMR-1 to 24.6 ± 27.5 grams at CMR-2 ($p < 0.001$). LV ejection fraction (average $68.5 \pm 9.4\%$) did not change significantly from CMR-1 ($p = 0.923$).

LGE extent increased (≥ 1 gram) in 44 patients (80%), with a mean increment of 11.3 ± 18.1 grams (median and IQR: 6 and 12 grams) (Figure 2). LGE extent unchanged (difference of LGE extent < 1 gram) in 6 patients and decreased in 2. Among the 11 patients without detectable LGE at CMR-1, eight patients showed ex-novo LGE at CMR-2 (Figure 3). Thus at CMR-2, LGE was globally found in 53 (96.4%) patients. In 15 patients (27.3%), the number of myocardial segments with LGE significantly increased from CMR-1 to CMR-2, while in 25 patients (45.5%), the increase of LGE was confined in the same segments of CMR-1. LGE-rate was 0.54 ± 0.98 (median and IQR: 0 and 1, range: 0–6) grams/month.

During the time interval between the CMR examinations, NYHA class improved from II to I class in 3 patients who started medical therapy after CMR-1, and worsened in 13 patients (10 from NYHA class I to II, 3 from class II to III). Therefore at CMR-2, twenty-three patients were in NYHA class II and 4 in class III.

LGE increment and clinical correlates

The increment of LGE extent (logarithmic values) between the two CMR scans was inversely related to the age at the enrolment ($r = -0.309$, $p=0.024$). The LGE increment was not correlated to the time interval between them ($r = 0.044$, $p=0.758$) and no difference was observed between males and females (12.2 ± 21.5 vs. 9.3 ± 6.8 , respectively, $p=0.592$).

Patients with apical HCM had a higher increment of LGE (9.4 ± 9.8 vs. 2.9 ± 3.1 % of LV mass, $p=0.004$) and LGE-rate (1.40 ± 1.78 vs. 0.33 ± 0.53 g/months, $p=0.001$) than those with other patterns of hypertrophy, despite a non-dissimilar increase in LV mass (32.0 ± 33.9 vs. 11.8 ± 31.0 g, $p=0.142$); in addition, there was no significant difference in the relationship between LGE at CMR-1 and LGE rate in the two groups (interaction term $p=0.818$). Patients with apical HCM had also a higher increment of LGE index by the LGE at CMR-1 (2.8 ± 3.0 vs. 0.9 ± 0.9 , $p=0.002$) than other patterns. Patients with worsening of NYHA class had higher increase of LGE extent (13.7 ± 10.8 vs. 6.1 ± 7.1 grams, $p=0.031$) and higher LGE-rate (1.15 ± 1.57 vs. 0.40 ± 0.51 grams/month, $p=0.049$) than those with preserved or improved clinical functional status.

A significant direct relationship between the increase of LV mass index and the increment of LGE was observed ($r=0.504$, $p<0.001$); furthermore, the increment of LGE was related to the extent of LGE at CMR-1 ($r=0.498$, $p<0.001$). Differently, LGE increase was not related to the LV mass index at CMR-1 ($p=0.352$), ejection fraction ($p=0.068$) and the maximal end-diastolic wall thickness ($p=0.077$).

The apical pattern of hypertrophy and the extent of LGE at CMR-1 were significant independent predictors of the increment of LGE between the examinations, in a multivariate model containing age as a covariate: the regression model overall explained almost 35% of the variability of LGE increase (Table 2). On average, having an apical pattern of hypertrophy would result in approximately 19 grams increase of LGE and 10 grams of LGE extent at CMR-1, would correspond to an average increase of approximately 4 grams at CMR-2.

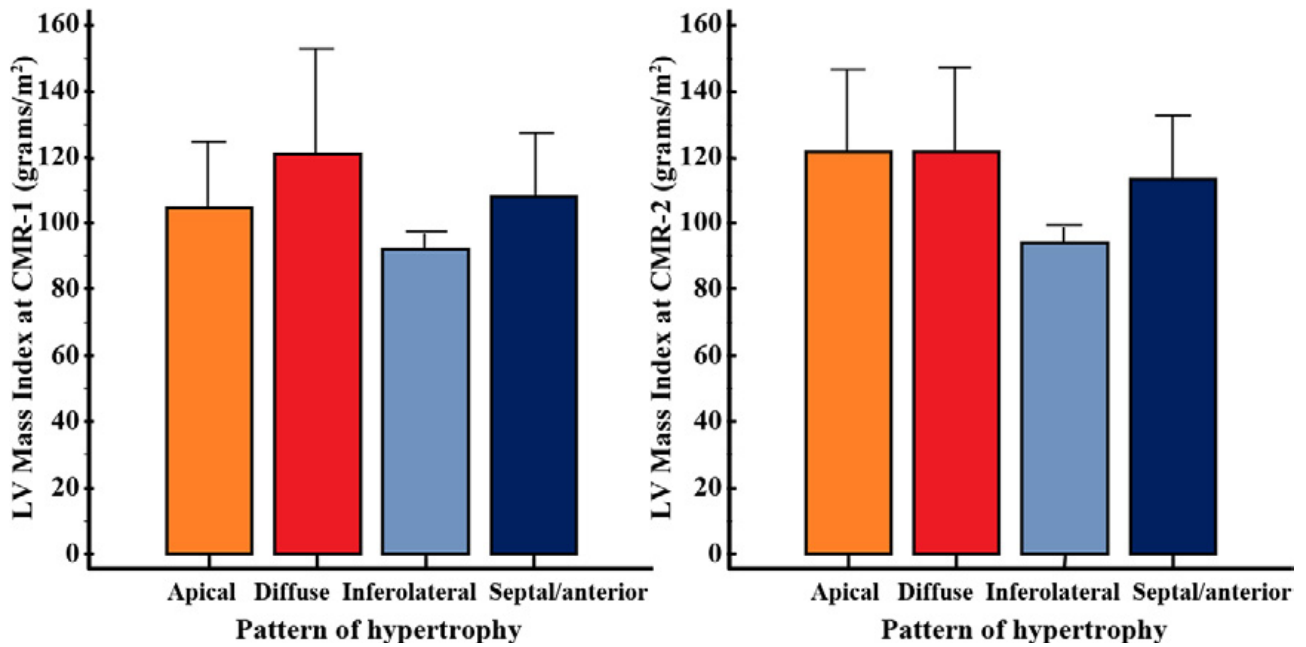


Figure 1: LV mass index at CMR 1 and CMR 2 in the different patterns of HCM

Left ventricular (LV) mass index was not significantly higher in patients with apical hypertrophic cardiomyopathy than in those with other patterns of hypertrophy at CMR-1 (left) and CMR-2 (right). CMR-1: first cardiac magnetic resonance examination; CMR-2 : second cardiac magnetic resonance examination.

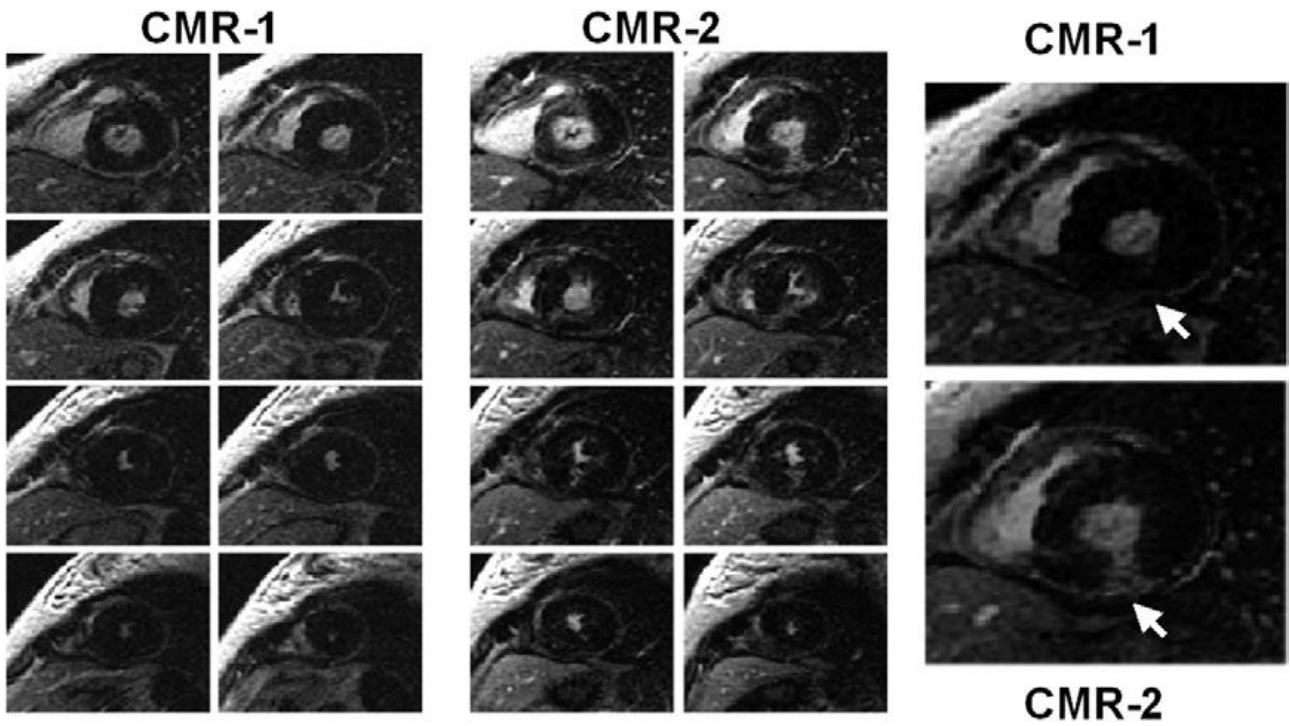


Figure 2: Apical hypertrophic cardiomyopathy at CMR

Late gadolinium enhancement (LGE) images of a patient with apical HCM at CMR-1 (left) and CMR-2 (right). Short- and long-axis images clearly show that the extent of LGE increased significantly. Abbreviations as in Figure 1.

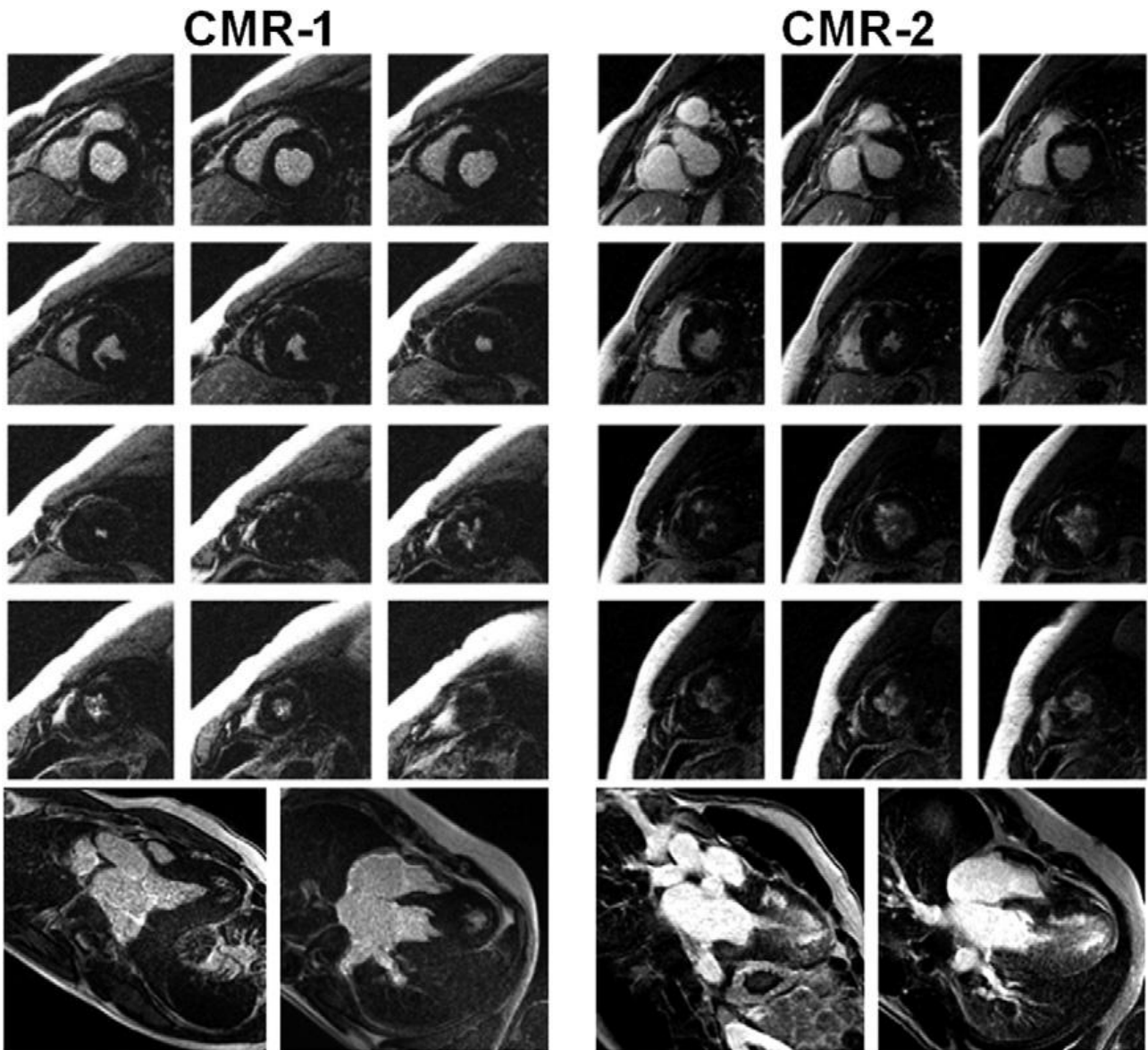


Figure 3: Diffuse hypertrophy at CMR

LGE images of a patient with diffuse hypertrophy at CMR-1 (left) and CMR-2 (right). At the first examination LGE was not detected, at CMR-2 LGE was detected in the anterior and lateral wall. Abbreviations as in Figures 1 and 2.

DISCUSSION

HCM is an evolutive disease, so it is intuitive to consider fibrosis a progressive phenomenon, however, the rate of progression of LGE was not previously evaluated. In this study we assessed for the first time the rate of progression of LGE by repeated CMR examinations in HCM patients. The main results were: a) after an average of two years the prevalence of LGE increase from 81.8% to 96.4% of subjects and the extent of LGE increased in the majority of them; b) subjects with apical HCM had greater increment of LGE and higher LGE-rate than those presenting other patterns of hypertrophy; c) the increment of LGE was higher in patients with NYHA class worsening.

The presence of LGE in patients with HCM may be considered relevant in terms of prognostic stratification, since recent reports demonstrated that after a clinical follow-up of three years patients with LGE had worse prognosis than those without LGE. However, the specificity of LGE as prognostic marker in HCM should be rediscussed because it is detected in most of the patients at the first evaluation and in almost all of them after few years as showed by these results. Then, the clinical and prognostic role of other features of LGE as its global extent, the pattern of distribution and the rate of progression should be evaluated by further studies in HCM patients.

In this study we evaluated the increment of LGE between two CMR examinations performed in a time range of 719 ± 410 days and calculated a new index, the LGE-rate, defined as the ratio between the increment of LGE in grams and the time in months between the two CMR examinations, which represents the rate of progression of LGE over time. LGE-rate was used to compare the progression of LGE extent in patients with a different time gap between the CMR examinations. However, results showed that the increment of LGE was not related to the time interval between the two CMR examinations and the rate of progression of LGE was highly heterogeneous with a spectrum of values of LGE-rate ranging from 0.06 to 2.53 g/month.

Although at CMR-1 the extent of LGE was not different in patients with different patterns of hypertrophy (figure 4), patients with apical HCM had higher increment of LGE and higher LGE-rate than other patterns of HCM at CMR-2 (figure 5). Moreover, at multiple regression analysis the apical pattern together with the extent of LGE at the first examination were independent predictors of the increment of LGE extent. In a case report, Gebker et al. described a large increment of LGE extent in patient with apical HCM between two CMR examinations after a time interval of two years. Several mechanisms may account for the higher progression of fibrosis in the apical pattern of LV hypertrophy. The physiological rarefaction of capillar density at the

ventricular apex, may participate to the mismatch between oxygen demand and supply in hypertrophic apical segments. In fact, Moon et al. demonstrated perfusion defect at the hypertrophied segment, representing abnormal myocardial capillary density, in apical HCM patients . In patients with apical HCM the development of apical aneurysm may be the extreme consequence of the increased fibrosis, shrinkage and severe wall thinning . Yet, myocardial infarction appears to be a common complication of apical HCM during long-term follow-up, even without significant CAD . Finally, a genetic predisposition may condition the rate of progression of fibrosis in apical as well in other patterns of HCM.

On the clinical point of view, a significant correlation between LGE and impaired functional class (NYHA class \geq II) was already demonstrated in previous reports . In addition, the current study showed a relation between the rate of progression of fibrosis and the clinical status: patients with worsened NYHA class had higher increment of LGE and LGE-rate than those with unchanged functional status. This result may be explained by the previous observation that impaired diastolic function was related to the extent of LGE in HCM and, consequently, a positive relation between the LGE-rate and the worsening of diastolic function may be hypothesized to justify the association between worsened NYHA and LGE-rate.

Main limitation of this study was the small size of population. This was expected, considering the percentage of HCM patients undergoing to ICD implantation after the first CMR and those with atrial fibrillation not permitting the acquisition of CMR images because of a non-optimal ECG triggering.

Another limitation was that the coronary artery angiography was performed only in patients with a positive exercise stress test. However, 36 patients, with a negative stress test, were aged <45 years and 17 of them were aged <30 years. The Framingham Risk score demonstrating a < 10% risk for coronary artery disease in all the remaining 16 patients . Furthermore, the pattern of distribution of LGE in all the patients in the two CMR examinations was not ischemic-like being intramural, patchy and non respecting the coronary vessel territory . Yet, in this study genetic analysis for the screening of sarcomeric mutations was not performed and further investigations are needed to assess whether the rate of progression of fibrosis may be conditioned by a genetic predisposition.

In conclusion, the progression of fibrosis in HCM is very fast, though very heterogeneous, and it is faster in apical hypertrophy than in other patterns and it is related to the worsening of the clinical status. Therefore CMR can be applied as an useful and safe tool, for longitudinal follow-up

evaluation of HCM. However, the clinical and prognostic impact of the LGE-rate, evaluated by repeated CMR examinations needs to be assessed by further studies, assessing also whether multiple CMR examination over time could be more useful than a “single shot” approach in the clinical setting.

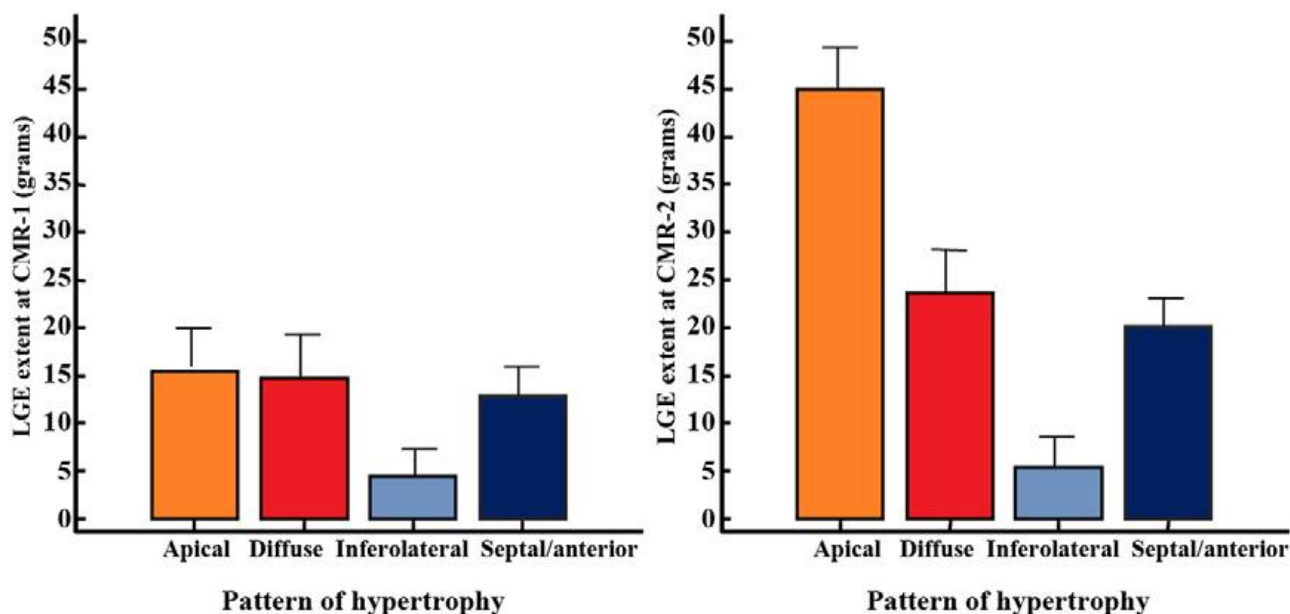


Figure 4: LGE in different pattern of hypertrophic cardiomyopathy

The histograms show the extent of LGE in the different patterns of hypertrophic cardiomyopathy at CMR-1 (left) and CMR-2 (right): patients with apical hypertrophy had higher extent of LGE at CMR-2. Abbreviations as in Figures 1 and 2.

Table 2: Multiple regression model for the prediction of increment of LGE extent at CMR-2.

Predictors	Total R ² = 0.348, p<0.001				
	Beta coef.	Beta (STD)	p-value	Partial R ²	
Age (years)	-0.172 (-0.419 to 0.075)	-0.168	0.168	2.6%	
Extent of LGE at CMR-1 (grams)	0.354 (0.072 to 0.636)	0.296	0.015	8.5%	
Apical pattern of HCM	18.63 (7.53 to 29.73)	0.400	0.001	15.1%	
Constant (grams)	10.47 (-2.42 to 23.36)	-	0.109	-	

LGE: Late Gadolinium Enhancement; CMR-1: first Cardiac Magnetic Resonance examination; HCM: Hypertrophic Cardiomyopathy. The extent of LGE at CMR-1 was expressed in grams, beta regression coefficients are reported as mean values with 95% CI.

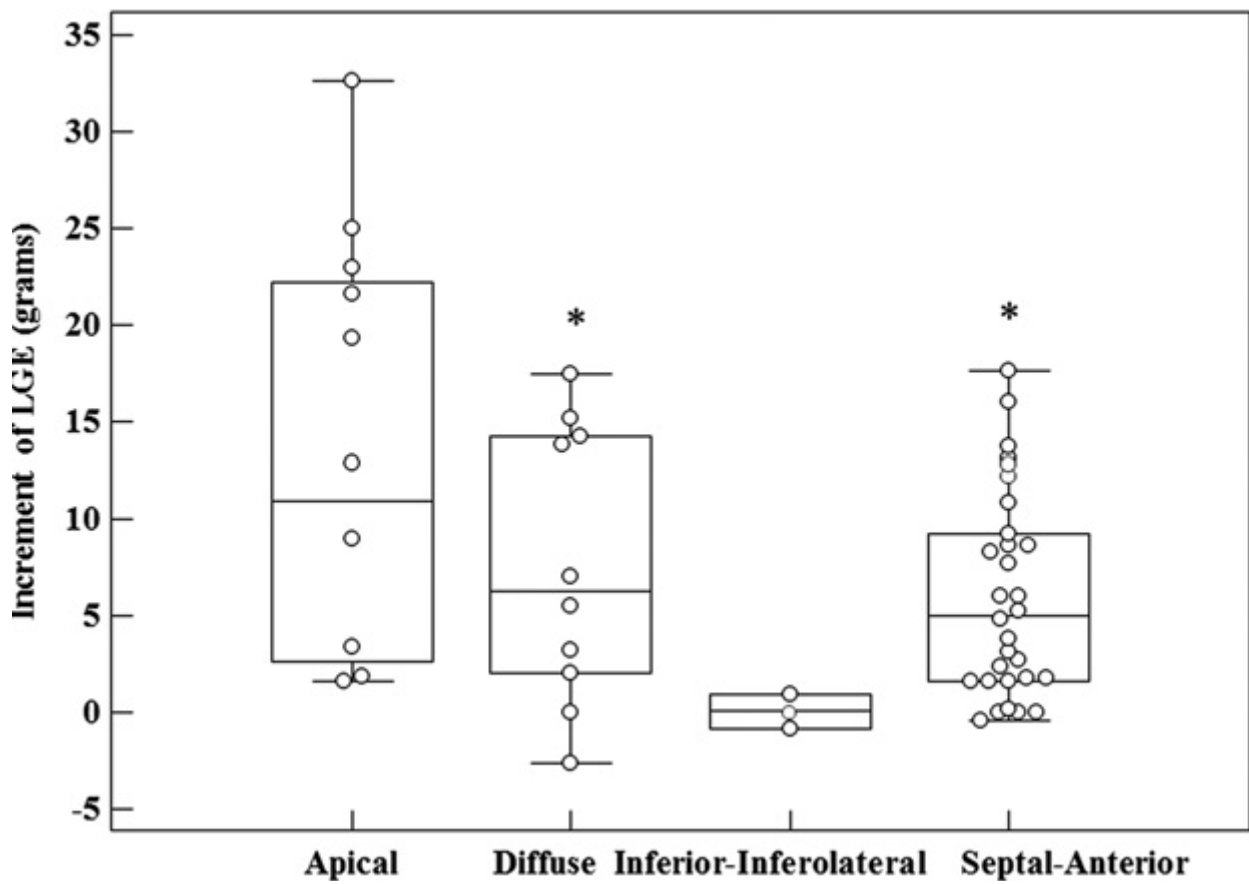


Figure 5: Increments of LGE

Box and whisker plot showing that the increment of LGE were significantly (*) higher in patients with apical pattern than those with diffuse hypertrophy or septal-anterior hypertrophy.

3) Myocardial abnormalities of T2-STIR magnetic resonance in Hypertrophic Cardiomyopathies: a predictor of electric myocardial instability.

(Unpublished data)

In the third study I have assessed the relationship between myocardial fibrosis, clinical status, expressed as arrhythmic instability, and tissue edema as sign of myocardial ischemia. Myocardial hyperintensity in T2-STIR images (HyT2) on CMR is usually considered as a marker of acute tissue damage, most frequently secondary to ischemic or inflammatory insult . HyT2 was also demonstrated in a proportion of patients with HCM . Melacini et al., comparing “first pass” perfusion, T2-Weighted (T2W) and LGE images, found that focal tissue abnormalities may consistent with regional ischemia at various stages: in the acute phase, the mechanisms leading to fibrosis are likely to be cell damage, “focal” edema, and cellular death whereas in the chronic phase, for example in patients with perfusion defects but without edema, LGE is mainly due to fibrosis, a tissue with an augmented interstitial matrix.

Considering that in HCM, myocardial ischemia due to microvascular disease was related to worse prognosis and it is considered as a trigger for arrhythmic events, the aim of my last third study was: 1) to prospectively evaluate the association between HyT2 and signs of ventricular electrical instability (premature ventricular contraction [PVC], NSVT, heart-rate variability) at 24h-Holter ECG monitoring and the arrhythmic risk score; 2) to compare HyT2 with other CMR-derived parameters as LGE presence, LGE extent, left ventricular mass index and maximal end-diastolic wall thickness.

METHODS

Patient Population

We enrolled consecutive patients with HCM who underwent a CMR examination. The diagnosis of HCM was based on previously-reported criteria (17). Sixty-eight HCM patients were consecutively enrolled for CMR exam. Out of these, 3 were excluded for low quality of CMR imaging and 1 for claustrophobia. Thus the final population consisted of 65 patients (51 males, 49 ± 17 years) who completed CMR examination. The study was approved by the ethical committees of our institutes. All patients received and signed informed consent.

Clinical evaluation

The presence of pre-existing conventional primary prevention risk markers for sudden death in HCM were evaluated: family history of sudden death, extreme left ventricular (LV) wall thickness

(> 30 mm), unexplained (non vasovagal) syncope, and non-sustained ventricular tachycardia (NSVT) on ambulatory Holter ECG recordings (> 3 ventricular beats at a heart rate > 120 beats per minute), abnormal "flat" systolic arterial pressure during exercise stress test .

A 24-hour Holter ECG monitoring was recorded in a time interval between three months before or after the execution of CMR examination. 24-h Holter ECG monitoring was recorded for conventional and time-domain analysis of heart rate variability: SD of RR intervals, SD of the average normal to normal QRS (NN) intervals calculated over periods of 5 min (SDANN); the number of interval differences of successive NN intervals >50 ms divided by the total number of NN intervals (pNN50); the square root of the mean squared differences of successive NN intervals (RMSSD) .

A complete clinical evaluation was performed in the day of CMR examination. By clinical interrogation, each patient was classified in a NYHA class on the basis of the presence and the severity of dyspnoea. The history of other symptoms (syncope, chest pain, palpitation) was also recorded. A 12-lead resting electrocardiogram was recorded on the day of the CMR scan.

CMR acquisition protocol

CMR was performed using two 1.5 Tesla system: a Signa Hdx (General Electric Healthcare, Milwaukee, Wisconsin) and a 1.5 Tesla Magnetom Avanto (Siemens, Erlangen, Germany) with cardiac phased array multichannel coils.

Short axis cine images from the mitral plane valve to the left ventricular apex were acquired using a steady state free precessing pulse sequence with the following parameters: 30 phases, slice thickness 8 mm, no gap, views per segment 8, NEX 1, FOV 40 cm, phase FOV 1, matrix 224x224, reconstruction matrix 256 x 256, a 45° flip angle, TR/TE equal to 3.5/1.5.

T2-STIR images were acquired using triple inversion recovery T2 weighted pulse sequence in short axis views and 2 long axis views (vertical and horizontal long axis view) using the following parameters: TR = 2 RR, TE ≈70 msec, FOV 40 cm, phase FOV 1, matrix 256 x 256, flip angle

LGE images were acquired starting 8 minutes after administration of Gd-DTPA (Magnevist, Schering-AG) with a dosage of 0.2 mmol/kg in short axis views. An inversion recovery T1-weighted GRE was used with the following parameters: field of view 40 mm, slice thickness 8 mm, no gap between each slice, repetition time 4.6 msec, echo time 1.3, flip angle 20°, matrix 224 x 224, reconstruction matrix 256 x 256, number of excitation 1. The appropriate inversion time was set to null normal myocardium (range 250-300 milliseconds).

Images post-processing

A commercially available research software package (Mass Analysis, Leyden, The Netherlands) was used for the quantification of functional parameters. Left ventricular (LV) mass was measured by the analysis of the cine short axis images. The endocardial and epicardial contours of LV myocardium were traced in the end-diastolic and the end-systolic phase. End-diastolic volume index (EDVi), end-systolic volume index (ESVi), mass and mass index were measured as previously described. LV mass index was considered severely increased when > 3 SD over upper limit of normality. Maximal LV end diastolic wall thickness was measured as previously described. T2-STIR images were evaluated using a qualitative visual assessment and also by a quantitative automatic analysis. The visual assessment was performed by three expert independent investigators blinded each others. The presence of signal abnormalities (HyT2) was established when there was agreement of evaluation in at least 2/3 investigators.

A complete agreement of the three investigators was reached in the analysis of the images of 95% patients. The quantitative evaluation was performed using a custom software. On short axis images a region of interest was placed in remote, non hypertrophied, myocardial segments and the mean signal intensity and standard deviation was measured in this region. Endocardial and epicardial contours were manually traced in short axis images and the signal intensity was measured in each voxel of images. A curve of distribution of signal intensity was automatically generated and myocardium was considered hyperintense when the signal intensity was higher than mean 2SD measured in the region interest. The extent of hyperintense myocardium in T2-STIR images was measured as the percentage of left ventricular mass.

The extent of LGE was measured using a previously validated method. Briefly, endocardial and epicardial contours in each image were manually traced to identify LV myocardium in each image. To obtain the standard deviation of the signal noise of the images a region of interest was placed in the background of the image, near the patient's thoracic wall. The mean signal intensity and standard deviation were measured in this region of interest.

Myocardial voxels with signal intensity higher than the average signal intensity of the region of interest plus 6 standard deviations were considered enhanced. The percentage of enhanced voxels in the entire LV myocardium was measured. Extent of LGE was expressed in gram and percentage of LV mass.

Statistical analysis

Categorical variables were compared by Pearson's chi-squared test with the continuity correction or Fisher's exact test when appropriate. The Kolmogorov-Smirnov test was used to assess normality of data. Pearson's (r) and Spearman's (p) correlation coefficients were employed for Gaussian and skewed variables, respectively. One-way analysis of variance (ANOVA) or Kruskal-Wallis test, when appropriate, were employed to compare quantitative variables between groups. Logistic regression analysis using a forward selection algorithm was used with the HyT2 as dependent variable, and LGE extent, left ventricular mass index, maximal end-diastolic wall thickness, LV ejection fraction and the number of arrhythmic risk factors as independent variables. Logistic regression analysis was also used to explore the impact of each variable in a model with the NSVT at 24-hour Holter ECG monitoring as dependent variable, and myocardial abnormalities at T2-STIR, LGE presence and LGE extent, left ventricular mass index, maximal end-diastolic wall thickness, LV ejection fraction and the number of arrhythmic risk factors (excluding NSVT) as independent variables.

A p-value <0.05 was considered to be statistically significant. Data are presented as continuous variables and proportions (percentages). Continuous variables are expressed as means \pm SD or median with interquartile range (IQR) as indicated.

RESULTS

Clinical findings

As evidenced in table 1, clinical expression was heterogeneous: 31 patients were symptomatic for effort dyspnea (26 in NYHA II, 5 in NYHA III); 13 angina; 26 palpitations; 6 syncope.

All the patients were in sinus rhythm during the examination; however, episodes of paroxysmal atrial fibrillation were reported in the clinical history of 16 patients (24%). None had severe valvular abnormalities.

As conventional risk factors for sudden cardiac death we found: 22 subjects (34%) presented non sustained ventricular tachycardia at 24-h Holter ECG monitoring, 11 (17%) familiar history of sudden death, and 8 (12%) a maximal end-diastolic wall thickness \geq 30 mm, none a significant drop of arterial blood pressure during exercise ECG. Thirty-six patients had no risk factors for sudden death, 18 presented one risk factor, while an arrhythmic risk score \geq 2 was found in 11 patients.

Table 1: Clinical characteristics of the population

		Global population	Hy-T2	No-HyT2	p value
Population	n(%)	65	27(42)	38(58)	
Age (years)	mean±SD	49 ± 17	52 ± 14	46 ± 17	0.59
Male	n(%)	51 (78)	22(81)	29(76)	0.84
LVOT obstruction	n(%)	15(23)	6(22)	9(24)	0.98
History of paroxysmal atrial fibrillation	n(%)	16(25)	8(30)	8(21)	0.59
Reduced ejection fraction (<50%)	n(%)	6(9)	5(19)	1(3)	0.08
Arrhythmic Risk Factors:					
Family history of SCD	n(%)	11(17)	5(19)	6(16)	0.97
VT at 24h Holter ECG monitoring	n(%)	22(34)	21(78)	1(3)	<0.001
Resuscitated SCD	n(%)	0	0	0	ns
Maximal wall thickness≥30	n(%)	8(12)	7(26)	1(3)	0.02
Unexplained Syncope	n(%)	6(9)	4(15)	2(5)	0.31
Outflow gradient >30 mmHg	n(%)	11(17)	4(15)	7 (18)	0.86
Abnormal pressure response during effort	n(%)	0	0	0	ns
Patients with 0 risk factors	n(%)	36(55)	3(11)	33(87)	<0.001
Patients with 1 risk factors	n(%)	18(28)	14(52)	4(11)	<0.001
Patients with≥2 risk factors	n(%)	11(17)	10(37)	1(3)	<0.001
Symptoms:					
Angina	n(%)	13(20)	7(26)	6(16)	0.42
Syncope	n(%)	6(9)	4(15)	2(5)	0.31
Palpitation	n(%)	26(40)	17(63)	9(24)	0.002
Dyspnea	n(%)	31(52)	10(37)	21(55)	0.18
NYHA class II	n(%)	26(40)	14(52)	12(32)	0.17
NYHA class III-IV	n(%)	5(8)	3(11)	2(5)	0.69
24h ECG Holter monitoring:					
	median(IQR)				
PVC)	37 (9-505)	33(14-1253)	41 (8-474)	0.74
NSVT	n(%)	22	21	1	<0.001
SDNN (ms)	mean±SD	130 ± 51	110 ± 38	154 ± 64	<0.01
SDANN (ms)	mean±SD	95 ± 25	86 ± 25	102 ± 21	0.02
pNNS0(%)	mean±SD	8 ± 5	9 ± 6	7 ± 5	0.15
RMSSD(ms)	mean±SD	49 ± 24	48 ± 17	50 ± 30	0.75
Therapy					
Beta-blockers	n(%)	35(54)	17(63)	18(47)	0.29
Calcium antagonist	n(%)	5(8)	4(15)	1(3)	0.13
ACE inhibitors	n(%)	17(26)	7(26)	10(26)	0.98
Antiarrhythmics	n(%)	15(23)	8(30)	7(18)	0.52

CMR findings

Summary of CMR results is reported in table 2.

LV mass index was increased in 44 patients (68%), and it was severely increased (> 3 SD of upper limit of normality) in 23 (35%). In six patients (9%), LV systolic dysfunction was found (range: 30-47%). In two patients (2%), LV dilation was found .

LGE was positive in 61 patients (93%) with a median extent of 9% of LV mass (IQR: 3-19%). Patients with positive LGE had higher end-diastolic wall thickness than those without (p=0.05).

A linear relation was found between the extent of LGE and LV mass index ($\rho=0.27$, $p=0.03$).

Table 2: CMR parameters

		Global population	Hy-T2	No-HyT2	p value*
Population	n(%)	65	27(42)	38(58)	
Age (years)	mean±SD	49 ± 17	52 ± 14	46 ± 17	
Male	n(%)	51(78)	22(81)	29(76)	0.84
Maximal Wall thickness (mm)	mean±SD	21 ± 6	25 ± 7	19 ± 5	<0.001
LV EDVi (ml/m ²)	mean±SD	73 ± 26	76 ± 35	71 ± 16	0.46
LV ESVi (ml/m ²)	mean±SD	24 ± 19	28 ± 27	20 ± 9	0.11
LV Mass index (g/m ²)	mean±SD	112 ± 40	133 ± 47	98 ± 28	<0.001
LV ejection fraction (%)	mean±SD	69 ± 12	66 ± 15	72 ± 8	<0.05
RV EDVi (ml/m ²)	mean±SD	65 ± 17	62 ± 18	67 ± 17	0.27
RV ESVi (ml/m ²)	mean±SD	19 ± 8	18 ± 9	19 ± 7	0.76
RV ejection fraction (%)	mean±SD	70 ± 7	70 ± 9	71 ± 5	0.63
LGE presence	n(%)	61(94)	26(96)	35(92)	0.86
LGE extent (% of LV mass)	mean±SD	11 ± 11	16 ± 12	7 ± 8	<0.001

T2-STIR , Holter ECG monitoring and clinical variables

On T2 STIR images HyT2 was detected in 27 patients (42%), with no sex ($p=0.62$) and age ($p=0.10$) differences (figure 1 and 2). HyT2 was detected in 3/36 (8%) of patients with no arrhythmic risk factor, in 14/18 (78%) of patients with one risk factor, in 7/8 (88%) of those with 2 risk factors and in 3/3 with 3 risk factors. By logistic regression analysis, the number of arrhythmic risk factor was the only predictor of HyT2 (odds ratio – OR: 19, from 5 to 70, $p<0.001$).

Subjects with HyT2 had higher LV mass index than those without (133 ± 47 vs 98 ± 28 g/m², $p<0.001$). The prevalence of HyT2 was higher in case of severely increased LV mass index (26% vs. 17%, $p=0.004$). LV EF was lower in patients with than those without HyT2 (66 ± 15 vs. $72 \pm 8\%$, $p=0.05$) and all the patients presenting with systolic dysfunction had HyT2.

Patient with HyT2 had greater extent of LGE than those without (16 ± 12 vs. 7 ± 8 % of LV mass, $p<0.001$).

At 24-h Holter ECG monitoring, 22 (27%) had episodes of NSVT. Patients with NSVT had higher LGE extent (18.3 ± 11.9 vs. 6.8 ± 7.9 % of LV mass, $p<0.001$), higher end-diastolic maximal wall thickness (25 ± 6 vs. 19 ± 6 mm, $p<0.001$), lower LV ejection fraction (64 ± 15 vs. 72 ± 8 % , $p=0.006$), higher LV mass index (131 ± 38 vs. 103 ± 39 , $p=0.007$) and more arrhythmic risk factors excluded TVNS (0.6 ± 0.7 vs. 0.14 ± 0.3 , $p=0.001$) than those without NSVT. Non-significant differences in age was found between those with and without NSVT ($p=0.14$).

Twenty-one patients with NSVT (95%) had HyT2 and only 6 patients with HyT2 had no NSVT at 24-h Holter ECG monitoring, then patients with HyT2 had higher prevalence of NSVT than those without ($p<0.001$) (figure 3).

The presence of myocardial enhancement at LGE images was not associated to occurrence of NSVT ($p=0.35$): 39 patients with a positive LGE (64%) had no NSVT but all the patients with NSVT had a positive LGE.

The SD of RR interval and SDANN at 24-hours Holter ECG monitoring were significantly lower in patients with HyT2 than those without (110 ± 38 vs. 154 ± 64 msec, $p<0.01$, and 102 ± 21 vs. 86 ± 25 , $p=0.02$, respectively).

By logistic regression analysis, HyT2 (OR: 165, 11-2455, $p<0.001$) and LGE-extent (1.1, 1.0-1.3, $p<0.001$) were independent predictors of NSVT at 24-h Holter ECG monitoring.

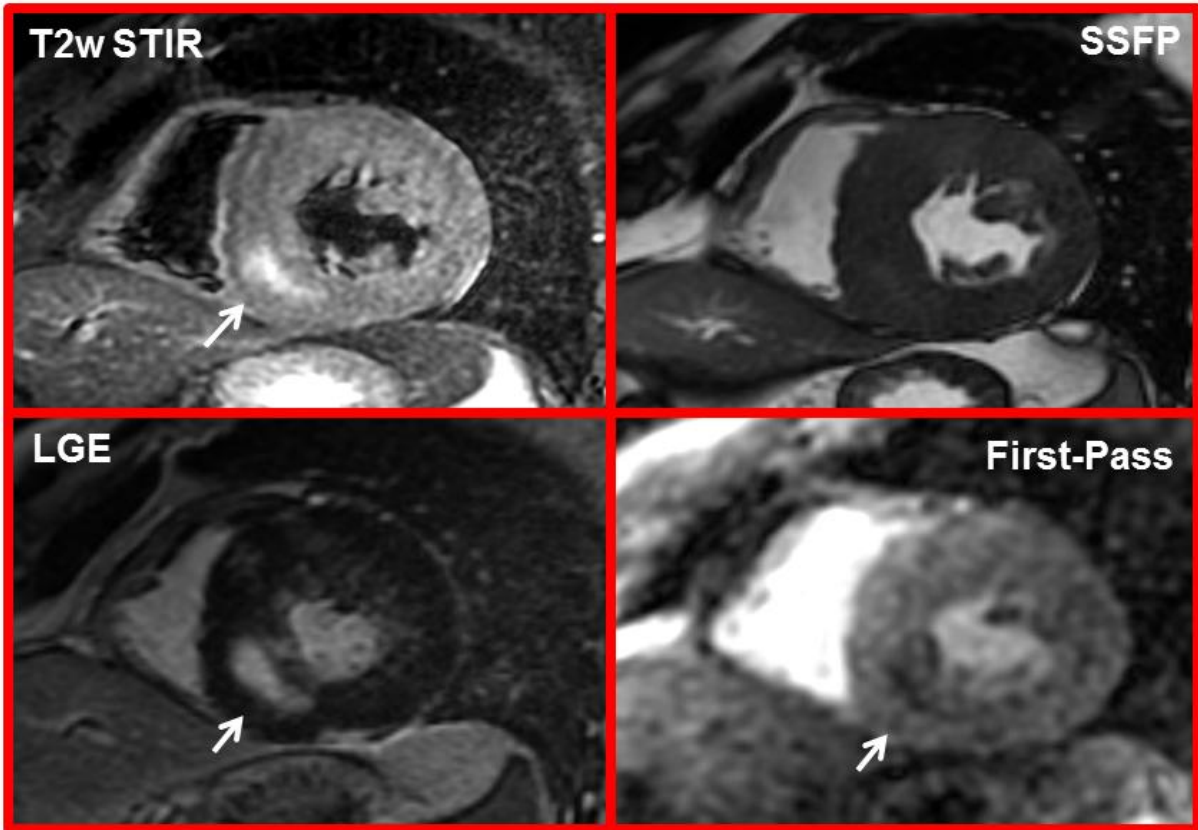


Figure 1. A case of a patient with HCM with HyT2 (arrow in T2-STIR images, left upper panel), myocardial fibrosis (arrow LGE images, left lower panel), and perfusion defect (arrow in the frame of the first pass gadolinium, right lower panel) in the same myocardial segments

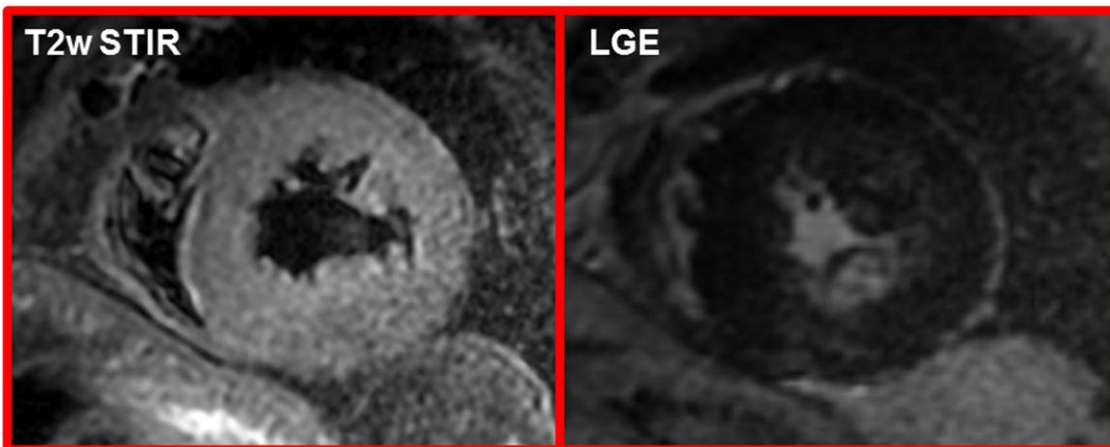


Figure 2: A case of a patient with HCM having myocardial fibrosis (LGE images, right panel) without HyT2 (T2-STIR images, left panel).



Figure 3: This patient with HyT2 (left upper panel) and myocardial fibrosis on LGE images (left lower panel) had a run of NSVT (right panel).

DISCUSSION

The main results of this study may be summarized as follows: 1) the presence of HyT2 was associated with signs of advanced disease consisting of higher LV mass index, lower ejection fraction and higher extent of LGE; 3) HyT2 was associated to a higher arrhythmic risk score; 4) HyT2 was associated to 24h Holter ECG monitoring parameters of electrical myocardial instability (NSVT and decreased heart rate variability); 5) among the CMR-derived parameters, HyT2 was the best predictor of NSTV.

These results suggest that the presence of myocardial edema in HCM patients is linked to the disease progression and electrical instability.

HyT2 was detected in 95% of patients with NSVT at 24-hours Holter ECG monitoring. In HCM the occurrence of NSVT at ambulatory Holter ECG monitoring is an important arrhythmic risk factor and it is also generally considered as marker of increased electric instability in cardiac diseases . The presence of HyT2 was also associated to decreased heart rate variability, suggesting a decreased vagal tone which leads to a superiority of sympathetic mechanism and cardiac electrical instability. A low heart rate variability was considered a marker of increased electrical instability and it was associated to increased risk of sudden cardiac death in ischemic and non-ischemic heart disease . It was previously demonstrated that a depressed heart rate variability was associated to arrhythmic events in HCM .

Etiology of HyT2

HyT2 was usually assumed as CMR sign of myocardial edema but its nature was not completely demonstrated . In ischemic heart disease myocardial HyT2 was usually considered as myocardial edema associated to a prolonged acute ischemic event, that not necessarily produces myocardial infarction . In fact, in the setting of acute myocardial infarction, necrotic myocardium was often surrounded by areas of transmural HyT2, which represent suffering but viable myocardium, and it is used for the assessment of myocardial salvage index . In myocarditis, HyT2 was considered a sign of active inflammation and it is usually located in sub-epicardial or in the midwall layer . HyT2 associated to myocardial infarction usually lasts for one month, whereas, when it is found in myocarditis, it may be detected also after 6 months.

In our HCM patients, HyT2 was located in the midwall of hypertrophic myocardial segments and it was coincident to areas with LGE. Previously, Melacini et al. hypothesized that these T2 abnormalities in HCM could be attributed to ischemia caused by microvascular disease, interstitial fibrosis, myocardial bridging, impaired diastolic relaxation and mismatch between capillary density

and myocardial tissue. In this setting prolonged ischemic events involving the hypertrophied myocardial segments may cause small intramural, rather than subendocardial, myocardial damage presenting at CMR with both HyT2 and LGE. HyT2 may be detectable in the acute/subacute phase but after it may potentially disappear, while LGE may persist as chronic scar. On other hand, Frustaci and colleagues found histopathological evidence of acute myocarditis in a significant fraction of their HCM cohort and related this finding to clinical deterioration : in these cases HyT2 may be expression of inflammatory myocardial damage. Therefore, HyT2 is a marker of acute ischemia and inflammation and both injuries are often associated to LGE and may constitute a trigger for arrhythmic events. However, the hypothesis of microvascular disease and ischemia as the cause of HyT2 is strongly supported by the observation that area of HyT2 closely matched with region of hypoperfusion at first pass of gadolinium CMR technique . Moreover, a global decrease of myocardial blood flow was previously demonstrated in HCM by CMR and PET studies . Particular, the extent of LGE was inversely related to the global myocardial blood flow suggesting a close relation between ischemic events and chronic myocardial damage . Repeating episodes of ischemia could partially explain the relatively fast progression of myocardial fibrosis in HCM, as recently demonstrated . In the current study we detected HyT2 in 42% of patients with HCM. Patients with HyT2 had higher LV mass index, lower ejection fraction and higher extent of LGE than those without. Moreover, patients with HyT2 had more arrhythmic risk factors than those without. All these findings suggest a more advanced disease in patient with HyT2 than in those without. Patients with higher LV mass index are more prone to have microvascular disease , a lower blood supply/demand ratio and increased interstitial fibrosis. These evidences suggest that in a more advanced stage of HCM, ischemic events may be more severe and prolonged than in early stages and potentially cause myocardial damages ranging from a reversible injury, presenting as HyT2, to an irreversible cell loss presenting with myocardial fibrosis and eventually depressing systolic function. All these factors may represent the substrate of electrical instability which may be triggered by a prolonged ischemic events depicted by HyT2 at CMR. As hypothesized in Coumel's triangle theory of arrhythmogenesis, myocardial disarray, fibrosis and hypertrophy are arrhythmogenic substrates that necessitate a trigger to induce arrhythmic events. The trigger for arrhythmic events may be a prolonged ischemic event, detected by CMR as HyT2.

HyT2 and LGE

The presence of LGE in patients with HCM may be considered relevant in terms of prognostic stratification. Recent reports demonstrated that after a clinical follow-up of 3 years, patients with

LGE had worse prognosis than those without LGE . However, LGE is usually detected in most of the HCM patients at the first CMR evaluation with a reported prevalence of 60-90% . Then, the specificity of LGE as prognostic marker in HCM should be rediscussed. Moreover, once fibrosis emerges in the heart its speed of expansion is a relatively fast phenomenon. Recently it was demonstrated that the progression of LGE extent is fast in an average follow-up of 2 years . Rate of progression of LGE was directly related to a worsening of the clinical outcome of the patients. Then, other features as the extent of LGE should be investigated. For this purpose, a recent multicenter trial demonstrated that the extent of LGE is a predictor of sudden cardiac death : the presence of extensive (>20% of left ventricular mass) and diffuse LGE was currently indicated as an emerging new arrhythmic risk factor . However, previous studies showed that an extent of LGE >20% of left ventricular mass was related to a loss of sufficient amount of contractile myocytes to worsen the systolic function and to contribute to the progression through end-stage disease . Results of the current study don't permit speculations about the long-term prognostic role of HyT2. However, HyT2 which is generally considered a sign of acute myocardial damage, may be considered a marker of acute arrhythmic risk. The detection of HyT2 may be potentially relevant for clinical management of patients with HCM. Patients with HyT2 may be considered at higher risk of arrhythmic events in the short-term period and maybe these patients could benefit by a close clinical surveillance. Further studies are needed to assess whether therapeutic adjustment may be driven by the detection of HyT2 at CMR. Yet, future studies should be performed to investigate about the evolution of HyT2 in HCM. Results of the current study showed a strict association between HyT2 and occurrence of NSVT at Holter ECG monitoring and it may be interesting to evaluate, by repeated CMR examinations, whether the disappearing of HyT2 might be also associated to disappearing of NSVT.

Limitations

Some limitations of the current study need to be addressed.

First, HyT2 may be detected in different conditions as ischemic events, inflammation and other acute causes of cardiac damage. Results of the current study do not allow to understand the nature and etiology of HyT2 in HCM. Then, the mechanism of the association between HyT2 and ventricular arrhythmias remains unclear.

Second, we assumed HyT2 in HCM as a sign of acute, transitory, myocardial damage but this assumption is based only by the observation of HyT2 in other cardiac disease. Then, further studies performing serial CMR examinations should be performed to confirm the reversibility of

HyT2 and the evolution of the association between HyT2 and acute electrical instability in HCM over time.

Finally, prognostic role of HyT2 was not evaluated in the current study and further investigations should be performed to assess the short- and long-term clinical impact of this CMR marker in larger HCM populations.

CONCLUSIONS

In patients with HCM the presence of HyT2 at CMR is associated to more advanced disease and it is linked to ventricular arrhythmias and to signs of electrical instability. HyT2 was detected in 42% of patients with HCM and it was the best predictor of NSVT at 24 Holter ECG monitoring. Yet, HyT2 was associated to depressed heart-rate variability and to a greater arrhythmic risk score.

Further studies are needed to assess the clinical and prognostic value of HyT2 in HCM and as well as also to understand its physiopathologic mechanism and the related potential therapeutical implications.

REFERENCES

1. Seidman CE, Seidman JG. Identifying sarcomere gene mutations in hypertrophic cardiomyopathy: a personal history. *Circ Res* 2011;108:743-50.
2. Maron BJ. Hypertrophic cardiomyopathy: A systematic review. *JAMA* 2002;287:1308-1320.
3. Maron BJ, Olivetto I, Spirito P et al. Epidemiology of Hypertrophic Cardiomyopathy–Related Death: Revisited in a Large Non–Referral-Based Patient Population. *Circulation* 2000;102:858-864.
4. Priori SG, Aliot E, Blomstrom-Lundqvist C et al. Update of the guidelines on sudden cardiac death of the European Society of Cardiology. *European Heart Journal* 2003;24:13-15.
5. Maron MS, Maron BJ, Harrigan C et al. Hypertrophic Cardiomyopathy Phenotype Revisited After 50 Years With Cardiovascular Magnetic Resonance. *Journal of the American College of Cardiology* 2009;54:220-228.
6. Shirani J, Pick R, Roberts WC, Maron BJ. Morphology and significance of the left ventricular collagen network in young patients with hypertrophic cardiomyopathy and sudden cardiac death. *Journal of the American College of Cardiology* 2000;35:36-44.
7. Maron BJ, Sato N, Roberts WC, Edwards JE, Chandra RS. Quantitative analysis of cardiac muscle cell disorganization in the ventricular septum. Comparison of fetuses and infants with and without congenital heart disease and patients with hypertrophic cardiomyopathy. *Circulation* 1979;60:685-96.
8. Harris KM, Spirito P, Maron MS et al. Prevalence, Clinical Profile, and Significance of Left Ventricular Remodeling in the End-Stage Phase of Hypertrophic Cardiomyopathy. *Circulation* 2006;114:216-225.
9. Olivetto I, Cecchi F, Casey SA, Dolara A, Traverse JH, Maron BJ. Impact of Atrial Fibrillation on the Clinical Course of Hypertrophic Cardiomyopathy. *Circulation* 2001;104:2517-2524.
10. Motoyasu M, Kurita T, Onishi K et al. Correlation between late gadolinium enhancement and diastolic function in hypertrophic cardiomyopathy assessed by magnetic resonance imaging. *Circulation journal : official journal of the Japanese Circulation Society* 2008;72:378-383.
11. Yacoub MH, Olivetto I, Cecchi F. 'End-stage' hypertrophic cardiomyopathy: from mystery to model. *Nat Clin Pract Cardiovasc Med* 2007;4:232-233.
12. Wigle ED, Rakowski H, Kimball BP, Williams WG. Hypertrophic Cardiomyopathy: Clinical Spectrum and Treatment. *Circulation* 1995;92:1680-1692.
13. McKenna WJ, Camm AJ. Sudden death in hypertrophic cardiomyopathy. Assessment of patients at high risk. *Circulation* 1989;80:1489-92.
14. Basso C, Thiene G, Corrado D, Buja G, Melacini P, Nava A. Hypertrophic cardiomyopathy and sudden death in the young: pathologic evidence of myocardial ischemia. *Human pathology* 2000;31:988-998.
15. Moon JC, Reed E, Sheppard MN et al. The histologic basis of late gadolinium enhancement cardiovascular magnetic resonance in hypertrophic cardiomyopathy. *Journal of the American College of Cardiology* 2004;43:2260-2264.
16. Bruder O, Wagner A, Jensen CJ et al. Myocardial scar visualized by cardiovascular magnetic resonance imaging predicts major adverse events in patients with hypertrophic cardiomyopathy. *J Am Coll Cardiol*;56:875-87.
17. O'Hanlon R, Grasso A, Roughton M et al. Prognostic significance of myocardial fibrosis in hypertrophic cardiomyopathy. *J Am Coll Cardiol*;56:867-74.
18. Aquaro GD, Positano V, Pingitore A et al. Quantitative analysis of late gadolinium enhancement in hypertrophic cardiomyopathy. *J Cardiovasc Magn Reson* 2010;12:21.
19. Maron MS, Olivetto I, Maron BJ et al. The case for myocardial ischemia in hypertrophic cardiomyopathy. *J Am Coll Cardiol* 2009;54:866-75.
20. Petersen SE, Jerosch-Herold M, Hudsmith LE et al. Evidence for microvascular dysfunction in hypertrophic cardiomyopathy: new insights from multiparametric magnetic resonance imaging. *Circulation* 2007;115:2418-25.

21. Kawada N, Sakuma H, Yamakado T et al. Hypertrophic cardiomyopathy: MR measurement of coronary blood flow and vasodilator flow reserve in patients and healthy subjects. *Radiology* 1999;211:129-35.
22. Bogazzi F, Lombardi M, Strata E et al. High prevalence of cardiac hypertrophy without detectable signs of fibrosis in patients with untreated active acromegaly: an in vivo study using magnetic resonance imaging. *Clinical endocrinology* 2008;68:361-368.
23. Van Rossum A, Visser F, Hofman M, Galjee M, Westerhof N, Valk J. Global left ventricular perfusion: noninvasive measurement with cine MR imaging and phase velocity mapping of coronary venous outflow. *Radiology* 1992;182:685-691.
24. Schwitter J, DeMarco T, Kneifel S et al. Magnetic resonance-based assessment of global coronary flow and flow reserve and its relation to left ventricular functional parameters: a comparison with positron emission tomography. *Circulation* 2000;101:2696-702.
25. Koskenvuo JW, Hartiala JJ, Knuuti J et al. Assessing coronary sinus blood flow in patients with coronary artery disease: a comparison of phase-contrast MR imaging with positron emission tomography. *American Journal of Roentgenology* 2001;177:1161-1166.
26. Anderson KM, Odell PM, Wilson PW, Kannel WB. Cardiovascular disease risk profiles. *American heart journal* 1991;121:293-298.
27. Lund GK, Wendland MF, Shimakawa A et al. Coronary Sinus Flow Measurement by Means of Velocity-encoded Cine MR Imaging: Validation by Using Flow Probes in Dogs¹. *Radiology* 2000;217:487-493.
28. Gatehouse PD, Rolf MP, Graves MJ et al. Flow measurement by cardiovascular magnetic resonance: a multi-centre multi-vendor study of background phase offset errors that can compromise the accuracy of derived regurgitant or shunt flow measurements. *J Cardiovasc Magn Reson* 2010;12:1.
29. Sechtem U, Pflugfelder P, Gould R, Cassidy M, Higgins CB. Measurement of right and left ventricular volumes in healthy individuals with cine MR imaging. *Radiology* 1987;163:697-702.
30. Vinnakota KC, Bassingthwaite JB. Myocardial density and composition: a basis for calculating intracellular metabolite concentrations. *Am J Physiol Heart Circ Physiol* 2004;286:H1742-9.
31. Kawaji K, Codella NC, Prince MR et al. Automated segmentation of routine clinical cardiac magnetic resonance imaging for assessment of left ventricular diastolic dysfunction. *Circulation: Cardiovascular Imaging* 2009;2:476-484.
32. Aquaro GD, Masci P, Formisano F et al. Usefulness of delayed enhancement by magnetic resonance imaging in hypertrophic cardiomyopathy as a marker of disease and its severity. *Am J Cardiol*;105:392-7.
33. Krams R, Kofflard M, Duncker D et al. Decreased coronary flow reserve in hypertrophic cardiomyopathy is related to remodeling of the coronary microcirculation. *Circulation* 1998;97:230-233.
34. Krams R, Ten Cate FJ, Carlier SG, van der Steen A, Serruys PW. Diastolic coronary vascular reserve: a new index to detect changes in the coronary microcirculation in hypertrophic cardiomyopathy. *Journal of the American College of Cardiology* 2004;43:670-677.
35. Wigle ED, Sasson Z, Henderson MA et al. Hypertrophic cardiomyopathy. The importance of the site and the extent of hypertrophy. A review. *Progress in cardiovascular diseases* 1985;28:1-83.
36. Spirito P, Bellone P, Harris KM, Bernabo P, Bruzzi P, Maron BJ. Magnitude of left ventricular hypertrophy and risk of sudden death in hypertrophic cardiomyopathy. *N Engl J Med* 2000;342:1778-85.
37. Elliott PM, Poloniecki J, Dickie S et al. Sudden death in hypertrophic cardiomyopathy: identification of high risk patients. *J Am Coll Cardiol* 2000;36:2212-8.
38. Adabag AS, Casey SA, Kuskowski MA, Zenovich AG, Maron BJ. Spectrum and prognostic significance of arrhythmias on ambulatory Holter electrocardiogram in hypertrophic cardiomyopathy. *J Am Coll Cardiol* 2005;45:697-704.
39. Maron BJ, Spirito P, Shen WK et al. Implantable cardioverter-defibrillators and prevention of sudden cardiac death in hypertrophic cardiomyopathy. *JAMA* 2007;298:405-12.

40. Olivotto I, Cecchi F, Gistri R et al. Relevance of coronary microvascular flow impairment to long-term remodeling and systolic dysfunction in hypertrophic cardiomyopathy. *J Am Coll Cardiol* 2006;47:1043-8.
41. Shewan LG, Coats AJ. Ethics in the authorship and publishing of scientific articles. *International journal of cardiology* 2010;144:1-2.
42. Maron BJ, McKenna WJ, Danielson GK et al. American College of Cardiology/European Society of Cardiology clinical expert consensus document on hypertrophic cardiomyopathy. A report of the American College of Cardiology Foundation Task Force on Clinical Expert Consensus Documents and the European Society of Cardiology Committee for Practice Guidelines. *J Am Coll Cardiol* 2003;42:1687-713.
43. Goldberger JJ, Cain ME, Hohnloser SH et al. American Heart Association/American College of Cardiology Foundation/Heart Rhythm Society Scientific Statement on Noninvasive Risk Stratification Techniques for Identifying Patients at Risk for Sudden Cardiac Death. A scientific statement from the American Heart Association Council on Clinical Cardiology Committee on Electrocardiography and Arrhythmias and Council on Epidemiology and Prevention. *J Am Coll Cardiol* 2008;52:1179-99.
44. Sechtem U, Pflugfelder P, Higgins CB. Quantification of cardiac function by conventional and cine magnetic resonance imaging. *Cardiovasc Intervent Radiol* 1987;10:365-73.
45. Maceira A, Prasad S, Khan M, Pennell D. Normalized left ventricular systolic and diastolic function by steady state free precession cardiovascular magnetic resonance. *Journal of Cardiovascular Magnetic Resonance* 2006;8:417-426.
46. Rickers C, Wilke NM, Jerosch-Herold M et al. Utility of cardiac magnetic resonance imaging in the diagnosis of hypertrophic cardiomyopathy. *Circulation* 2005;112:855-61.
47. Harrigan CJ, Peters DC, Gibson CM et al. Hypertrophic cardiomyopathy: quantification of late gadolinium enhancement with contrast-enhanced cardiovascular MR imaging. *Radiology* 2011;258:128-133.
48. Adabag AS, Maron BJ, Appelbaum E et al. Occurrence and frequency of arrhythmias in hypertrophic cardiomyopathy in relation to delayed enhancement on cardiovascular magnetic resonance. *J Am Coll Cardiol* 2008;51:1369-74.
49. Gebker R, Neuss M, Paetsch I, Nagel E. Images in cardiovascular medicine. Progressive myocardial fibrosis in a patient with apical hypertrophic cardiomyopathy detected by cardiovascular magnetic resonance. *Circulation* 2006;114:e75-6.
50. Moon J, Cho IJ, Shim CY et al. Abnormal myocardial capillary density in apical hypertrophic cardiomyopathy can be assessed by myocardial contrast echocardiography. *Circ J*;74:2166-72.
51. Kubo T, Kitaoka H, Okawa M et al. Clinical profiles of hypertrophic cardiomyopathy with apical phenotype--comparison of pure-apical form and distal-dominant form. *Circ J* 2009;73:2330-6.
52. Matsubara K, Nakamura T, Kuribayashi T, Azuma A, Nakagawa M. Sustained cavity obliteration and apical aneurysm formation in apical hypertrophic cardiomyopathy. *J Am Coll Cardiol* 2003;42:288-95.
53. Maron MS, Finley JJ, Bos JM et al. Prevalence, clinical significance, and natural history of left ventricular apical aneurysms in hypertrophic cardiomyopathy. *Circulation* 2008;118:1541-9.
54. Eriksson MJ, Sonnenberg B, Woo A et al. Long-term outcome in patients with apical hypertrophic cardiomyopathy. *J Am Coll Cardiol* 2002;39:638-45.
55. Maron MS, Appelbaum E, Harrigan CJ et al. Clinical profile and significance of delayed enhancement in hypertrophic cardiomyopathy. *Circ Heart Fail* 2008;1:184-91.
56. Wilson PW, D'Agostino RB, Levy D, Belanger AM, Silbershatz H, Kannel WB. Prediction of coronary heart disease using risk factor categories. *Circulation* 1998;97:1837-47.
57. Soriano CJ, Ridocci F, Estornell J, Jimenez J, Martinez V, De Velasco JA. Noninvasive diagnosis of coronary artery disease in patients with heart failure and systolic dysfunction of uncertain etiology, using late gadolinium-enhanced cardiovascular magnetic resonance. *J Am Coll Cardiol* 2005;45:743-8.

58. Melacini P, Corbetti F, Calore C et al. Cardiovascular magnetic resonance signs of ischemia in hypertrophic cardiomyopathy. *International journal of cardiology* 2008;128:364-373.
59. Abdel-Aty H, Cocker M, Strohm O, Filipchuk N, Friedrich MG. Abnormalities in T2-weighted cardiovascular magnetic resonance images of hypertrophic cardiomyopathy: Regional distribution and relation to late gadolinium enhancement and severity of hypertrophy. *Journal of Magnetic Resonance Imaging* 2008;28:242-245.
60. Cecchi F, Olivotto I, Gistri R, Lorenzoni R, Chiriatti G, Camici PG. Coronary microvascular dysfunction and prognosis in hypertrophic cardiomyopathy. *N Engl J Med* 2003;349:1027-35.
61. Frenneaux MP. Assessing the risk of sudden cardiac death in a patient with hypertrophic cardiomyopathy. *Heart* 2004;90:570-5.
62. Camm A, Malik M, Bigger J et al. Heart rate variability: standards of measurement, physiological interpretation and clinical use. Task Force of the European Society of Cardiology and the North American Society of Pacing and Electrophysiology. *Circulation* 1996;93:1043-1065.
63. Doval HC, Nul DR, Grancelli HO et al. Nonsustained Ventricular Tachycardia in Severe Heart Failure Independent Marker of Increased Mortality due to Sudden Death. *Circulation* 1996;94:3198-3203.
64. Pelliccia F, Gallo P, Cianfrocca C, d'Amati G, Bernucci P, Reale A. Relation of complex ventricular arrhythmias to presenting features and prognosis in dilated cardiomyopathy. *International journal of cardiology* 1990;29:47-54.
65. Ikegawa T, Chino M, Hasegawa H et al. Prognostic significance of 24-hour ambulatory electrocardiographic monitoring in patients with dilative cardiomyopathy: A prospective study. *Clinical cardiology* 1987;10:78-82.
66. La Rovere M, Pinna G, Hohnloser S et al. Autonomic tone and reflexes after myocardial infarction. Baroreflex sensitivity and heart rate variability in the identification of patients at risk for life-threatening arrhythmias: implications for clinical trials. *Circulation* 2001;103:2072-2077.
67. Uemura S, Tomoda Y, Fujimoto S et al. Heart rate variability and ventricular arrhythmia in clinically stable patients with hypertrophic cardiomyopathy. *Japanese circulation journal* 1997;61:819.
68. Willerson JT, Scales F, Mukherjee A et al. Abnormal myocardial fluid retention as an early manifestation of ischemic injury. *The American journal of pathology* 1977;87:159.
69. Friedrich MG, Abdel-Aty H, Taylor A, Schulz-Menger J, Messroghli D, Dietz R. The salvaged area at risk in reperfused acute myocardial infarction as visualized by cardiovascular magnetic resonance. *Journal of the American College of Cardiology* 2008;51:1581-1587.
70. Friedrich MG, Sechtem U, Schulz-Menger J et al. Cardiovascular magnetic resonance in myocarditis: a JACC white paper. *Journal of the American College of Cardiology* 2009;53:1475-1487.
71. Frustaci A, Verardo R, Caldarulo M, Acconcia MC, Russo MA, Chimenti C. Myocarditis in hypertrophic cardiomyopathy patients presenting acute clinical deterioration. *European heart journal* 2007;28:733-740.
72. Aquaro GD, Todiere G, Barison A et al. Myocardial blood flow and fibrosis in hypertrophic cardiomyopathy. *Journal of Cardiac Failure* 2011;17:384-391.
73. Todiere G, Aquaro GD, Piaggi P et al. Progression of myocardial fibrosis assessed with cardiac magnetic resonance in hypertrophic cardiomyopathy. *Journal of the American College of Cardiology* 2012;60:922-929.
74. Aquaro GD, Masci P, Formisano F et al. Usefulness of delayed enhancement by magnetic resonance imaging in hypertrophic cardiomyopathy as a marker of disease and its severity. *Am J Cardiol* 2010;105:392-7.
75. Maron MS. Clinical utility of cardiovascular magnetic resonance in hypertrophic cardiomyopathy. *J Cardiovasc Magn Reson* 2012;14:13.
76. Chan RH, Maron B, Assenza G et al. Prognostic utility of contrast-enhanced cardiovascular magnetic resonance in hypertrophic cardiomyopathy: an international multicenter study. *Journal of the American College of Cardiology* 2012;59:E1570-E1570.
77. Maron BJ, Maron MS. Hypertrophic cardiomyopathy. *The Lancet* 2013;381:242-255.

78. Olivotto I, Maron BJ, Appelbaum E et al. Spectrum and clinical significance of systolic function and myocardial fibrosis assessed by cardiovascular magnetic resonance in hypertrophic cardiomyopathy. *The American journal of cardiology* 2010;106:261-267.
79. Olivotto I, Cecchi F, Poggesi C, Yacoub MH. Patterns of Disease Progression in Hypertrophic Cardiomyopathy: An Individualized Approach to Clinical Staging. *Circulation: Heart Failure* 2012;5:535-546.